1967

The engineering properties of cohesionless materials during vibration

Thomas Leslie Youd
Iowa State University

YOUD, Thomas Leslie, 1938-
THE ENGINEERING PROPERTIES OF COHESIONLESS MATERIALS DURING VIBRATION.

Iowa State University, Ph.D., 1967
Engineering, civil

University Microfilms, Inc., Ann Arbor, Michigan

THE ENGINEERING PROPERTIES OF COHESIONLESS MATERIALS DURING VIBRATION

by

Thomas Leslie Youd

A Dissertation Submitted to the
Graduate Faculty in Partial Fulfillment of
The Requirements for the Degree of
DOCTOR OF PHILOSOPHY

Major Subject: Soil Engineering

Approved:

Signature was redacted for privacy.

In Charge of Major Work

Signature was redacted for privacy.

Head of Major Department

Signature was redacted for privacy.

Dean of Graduate College

Iowa State University
of Science and Technology
Ames, Iowa

1967

TABLE OF CONTENTS

I. INTRODUCTION

Earthquakes, blasts, high speed traffic, and a multitude of reciprocating and pulsating machines are sources for vibrations which propagate through soils. Several of the basic engineering properties of soils, such as density, shear strength and permeability, are susceptible to vibration (Barkan, 1962). Since these soil properties are used by the engineer in designing foundations, bases, embankments, and determining the safety of existing earth masses against failure, an understanding of the effect of shocks and vibration on these properties is essential to the design engineer.

Soils which were stable under static conditions have failed when subjected to vibrations. Five major slope failures occurred in Anchorage, Alaska, as a result of the March, 1964, earthquake (Idriss, 1967). During the Nigata, Japan, earthquake of June 16, 1964, many structures settled more than three feet and one apartment building rotated through an angle of eighty degrees (Seed, 1967). Catastrophic failures of this type, unfortunately, have had a high frequency of occurrence. Less catastrophic but still problematic are settlements in soils adjacent to bridge abutments or under vibrating equipment.

Vibration of soil can also be beneficial as in compaction of granular soils. Field investigations have shown that for certain types of soil, higher densities and greater depths of compaction have been obtained with vibratory compactors than with heavier static compactors (Johnson, 1960). Vibration is also one of the main factors causing densification by the patented processes of "Vibroflotation" (D'Appolonia, 1953) and compaction

with explosives (Goodman, 1965).

Although an understanding of the effect of vibration on the mechanical properties of soil is essential for safe engineering design, only a limited amount of knowledge is presently available on many of these effects. Linger (1963) stated, "After a review of the literature available on the subject of soil vibration, it could be concluded that not much 'basic' research has been done and, as a result, more studies should be made to isolate and study the basic dynamic properties of soil."

In answer to this need for a better understanding of the behavior of soil when subjected to vibration, a research program on the effect of vibration on the stability of granular soils was started in 1964. The objectives of this investigation were:

1. To investigate the reduction of shear strength during vibration.
2. To investigate the effect of vibration on the void ratio during shear failure, including the effect on the critical void ratio.
3. To investigate the relationship between density and frequency and amplitude of vibration.

II. REVIEW OF LITERATURE

A. Shear Strength of Granular Soils

Depending on the source of its strength soil can be classified as either cohesive or cohesionless. Cohesive soils are those in which the surface forces of the soil particles are largely responsible for the soil strength (Scott, 1963). Since the materials used in this investigation were cohesionless, no further mention will be made of cohesive soils.

Two factors contribute to the shear strength of cohesionless soils. One factor is the frictional resistance which is a combination of sliding and rolling resistances as particles slide or roll past one another. This factor is referred to as friction (Taylor, 1948). The second factor is due to the interlocking of particles. Historically, interlocking has been considered to be a part of the frictional resistance; thus the total shearing resistance, which is the sum of both factors, is termed the internal friction (Taylor, 1948).

1. Friction

The first known written remarks on the nature of friction were by Leonardo da Vinci. He proposed that the frictional resistance between two sliding bodies was proportional to the normal force and independent of the area of contact between the surfaces (reported by Mac Curdy, 1938).

Amontons (1699) formulated laws relating frictional resistance and the normal force acting on a body sliding on a surface. He stated that the shearing force S is proportional to the normal force N,

$$S = fN \qquad (1)$$

where f is a constant of proportionality called the coefficient of friction. This is known as Amontons second law and it has been found to be valid over a wide range of experimental conditions (Bowden, 1950). Coulomb (1781) later confirmed the laws of Amontons.

The mechanism of friction between solids has been clarified in recent years. Terzaghi (1925) proposed that the frictional force developed between two unlubricated surfaces was the result of molecular bonding at the real area of contact. He further proposed that the real area of contact was proportional to the normal load and that the shear strength at the contact is independent of the normal load. These relationships are formulated as follows:

$$S = A's' \tag{2}$$

$$f = s'/p \tag{3}$$

where: S = the frictional resistance

A'= the real area of contact

s'= the shear strength per unit area of the molecular bonds

f = the coefficient of friction

p = the normal pressure per unit area of real contact

Bowden and Tabor (1950) working with metals, confirmed Terzaghi's hypothesis that the area of real contact is proportional to the normal load. They found that under any level of applied normal load plastic yielding takes places at the contact between asperities, thus the real area of contact is

$$A' = N/p \tag{4}$$

where p is the contact pressure at the real area of contact and also the yield pressure of the metal. They also found that adhesion takes place between the two bodies at the points of real contact, and that the force necessary to shear the junctions at the real contacts is proportional to the area of the contact.

Another mechanism associated with the friction between solids is "junction growth" described by Tabor (1959). He showed that as the tangential force was gradually increased from zero, the area of real contact increased, reaching a maximum when slippage was imminent. This maximum was up to several times (for hard clean metals) the initial contact area with no change in normal force. However, the final contact area was found to be a constant times the initial contact area, thus maintaining the proportionality between tangential and normal forces when slippage occurred.

Eyring and Powell (1944) gave the following mechanism of friction for two unlubricated surfaces moving past each other: the surfaces of even optically smooth metals have irregular hills and valleys 500 to 1000 atom diameters deep. The surfaces also have smaller periodic valleys between each atom. The tangential force necessary to cause sliding thus is composed of three components: one component to supply the work to raise one surface over the gross irregularities, the second to raise the surface over the atomic irregularities, and the third to break the bonds produced by plastic deformation of the surface. Yong and Warkentin (1966) attribute sliding frictional resistance to the first two of these three factors, namely surface roughness, which they term as microscopic interlocking and note that there is no significant volume change associated with this action.

In summary, the adhesional theory is now generally accepted as being valid for both metallic and non-metallic surfaces. In addition microscopic interlocking also contributes to the frictional resistance of "rough" surfaces. Rolling resistance has in general either been combined with sliding friction or neglected. Tinoco (1967) concluded from an energy study on the failure mechanism of cohesionless soils that resistance to sliding was the principal factor in the frictional resistance.

2. Interlocking

Reynolds (1885) found that dense sands expand during shear failure, a phenomenon he called dilatancy. He also found that loose sands contracted during failure. This dilatancy is due to interlocking of particles, and may be explained in the following manner. When one particle is lodged in a depression between other particles, it will have to be lifted out of the depression in order for shear displacement to occur. Since the motion of individual particles in such a case has a component normal to the plane of failure, the volume of the sample increases during failure. Furthermore, a considerable amount of the work required to produce failure is used in expanding the sample against the applied normal stress (Taylor, 1948). By measuring the volume changes during a direct shear test on sand, Taylor (Ibid.) was able to separate the energy required to shear the sample into two components. The work done against dilatancy or interlocking is the product of the thickness increase and the normal load on the sample. By subtracting this energy from the total energy expended in shear the energy component due to friction is determined. Formulated in terms of frictional coefficients this separation becomes (Leonards, 1962),

$$\tan\phi_r = \tan\phi - \frac{\Delta h}{\Delta \delta} \qquad (5)$$

where: $\tan\phi_r$ = the coefficient of friction

$\tan\phi$ = the coefficient of internal friction

Δh = the change in sample height due to an incremental shear displacement $\Delta\delta$

3. Critical void ratio

In general, deformation of a cohesionless soil results in a volume change. If the soil is very loose, particles will fall into holes during deformation, resulting in a net volume decrease, whereas if the soil is dense, dilatation will occur during shear as particles are displaced normal to the shear plane. Since deformation in dense sands produces a volume increase and deformation in loose sands produces a volume decrease, there must be some intermediate density where deformation produces no net volume change. This density is referred to as critical density, and the corresponding void ratio as the critical void ratio.

It has been shown (Means, 1963) (Roscoe, 1958) that for a given loading condition a sample approaches the critical void ratio when sheared to the ultimate state. Figure 1 was taken from the results of Roscoe (1958) and co-workers and clearly shows that the samples they tested either dilated or contracted, as the case may be, to approach a void ratio near the value of the critical void ratio.

The definition of the critical void ratio in this case is that given by Roscoe for a drained shear test.

> In a drained test the critical voids ratio state can be defined as that ultimate state of a sample at which any arbitrary further increment of shear distortion will not result in any change in voids ratio.

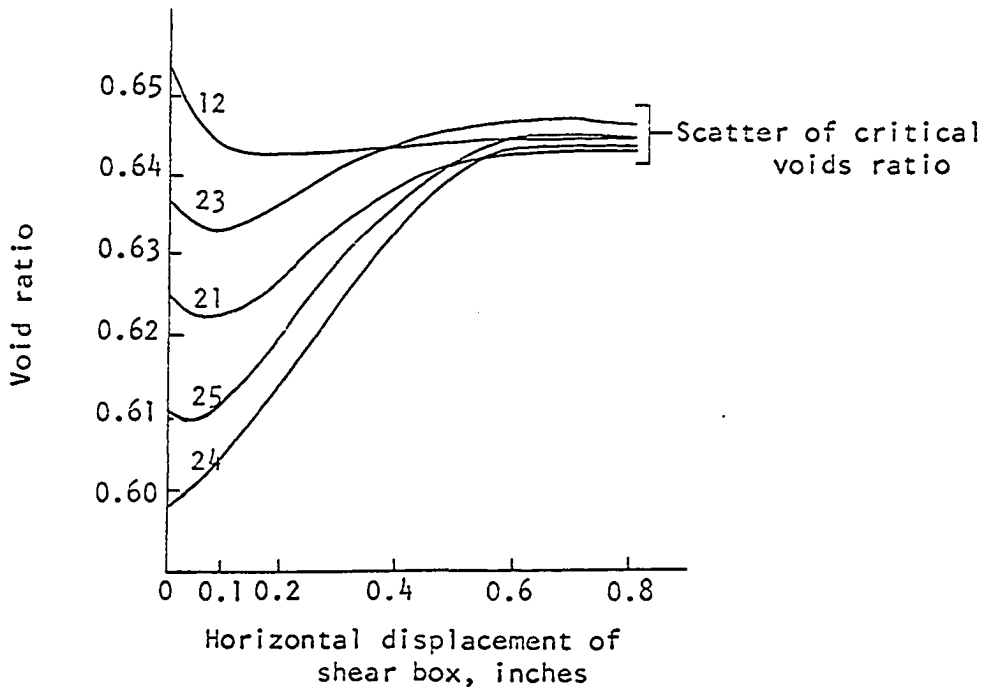

Figure 1. Results of simple shear tests on 1-mm steel balls with normal stress - 20 lb/sq. in. After Roscoe, et al.(1958)

This is the definition of critical void ratio that shall be used in this thesis. The term critical void ratio is abbreviated by the initials CVR.

At least three other definitions of the CVR have been given. They are summarized in Taylor (1948) as follows:

1. Casagrande CVR.

Values of Casagrande critical void ratios are determined by

a series of constant-σ_3 cylindrical compression tests of conventional type with individual tests at a number of σ_3 values and at various densities. The void ratio of each specimen is determined before it is placed under lateral pressure for testing. For each specimen the resulting volume change between the start of the test and the peak point .... is obtained. For the various tests at a given σ_3 value, the void ratio before loading is plotted against the resulting volume change. On this plot the void ratio at the point of zero volume change may be read off, and this void ratio is the desired critical void ratio.

2. Constant-σ_3 CVR

   In the determination of the constant-σ_3 critical void ratio the recorded initial void ratio of each test is the value holding at the start of the test just after the σ_3 value of the test has been applied, whereas the Casagrande critical void ratio is based on the initial void ratio before loading.

3. Constant-volume CVR

   To obtain this critical void ratio, a series of constant volume cylindrical compression tests are run at various initial-σ_3 values and at various densities. For the several tests at each initial-σ_3 value, the σ_3 value attained at the peak point is plotted against the void ratio of the test. At the point where the ordinate equals the initial-σ_3 value, the abscissa is the constant-volume critical void ratio.

Although the differences in these definitions may appear small they are very important and illustrate the care that must be used in defining the CVR.

The CVR is not a constant for any given material, but is a function of the applied stresses (Roscoe, 1958). Scott (1963) states that the value of the CVR also depends on the type of test used and the stage of the experiment at which the void ratio is determined.

B. Vibrational Effects on Shear Strength

One of the first investigators to note that the coefficient of internal friction was reduced during vibration was Krey (1932). Experimenting with rye grain and with sand, he found that the angle of repose

was reduced by vibration. (The angle of repose is one of the oldest and simplest methods of estimating the angle of internal friction.) Thus Krey concluded that the internal friction was reduced during vibration.

An extensive investigation of the vibrational effects on the properties of sands was carried out by Pokrovsky and Barkan and associates (Barkan, 1962). They conducted shear tests similar in principle to those of this investigation using a stress-controlled direct shear device mounted on a vibrator. The normal load was applied by a spring mechanism, and the shear load was applied by a cable passing over a pulley-shock absorber mechanism to a loading platform. The shear load was then applied by placing weights on the platform. The direction of table motion was in the direction of shear. The vibrator used was adjustable with frequencies up to 50 cps and amplitudes up to 1.7 mm (0.067 in.).

The tests were made by filling the shear box with sand and placing it on the vibratory platform. Then the sand was compacted by means of vibrations under a normal pressure of 0.5 kg/cm^2 (7.0 psi). After that the pressure on the soil was increased to the magnitude of the test and shearing of the soil was induced while the box was vibrated at preselected amplitudes and frequencies.

No quantitative observations on void ratio values were reported from the investigations. However, Barkan noted that with an increase in shear load the samples first contracted and then began a process of expansion. They also found that the change in porosity due to shear decreased with increasing normal load.

These investigators conducted shear tests, both static and while subjected to vibration, studying the effects of frequency and amplitude of

vibration on the reduction of the coefficient of internal friction. They found that the friction angle was reduced by both frequency and amplitude. They then plotted the results against the acceleration ratio, η, where

$$\eta = \frac{\omega^2 a}{g} \tag{6}$$

$\omega^2 a$ = the maximum acceleration of vibration

ω = the frequency of vibration

a = the amplitude of vibration

g = the acceleration of gravity

A reproduction of these results is shown in figure 2 where $\tan\phi$ is the coefficient of internal friction and the data points shown represent a variety of amplitudes and frequencies. From these results Barkan formulated an empirical equation relating $\tan\phi$ to the acceleration ratio, η:

$$\tan\phi = \tan\phi_{\infty} + (\tan\phi_{st} - \tan\phi_{\infty})\underline{e}^{-\beta\eta} \tag{7}$$

$\tan\phi_{\infty}$ = the minimum limit value of $\tan\phi$

$\tan\phi_{st}$ = the static value of $\tan\phi$

β = a coefficient

$\underline{e}$ = the base of natural logarithms

Barkan listed the value of β as 0.23 for dry medium-grained sand.

Barkan also investigated the effect of grain size on the reduction of internal friction by vibration. Results of these tests are shown in figure 3, where δ is defined as

$$\delta = \frac{\tan\phi_{st} - \tan\phi}{\tan\phi_{st}} \tag{8}$$

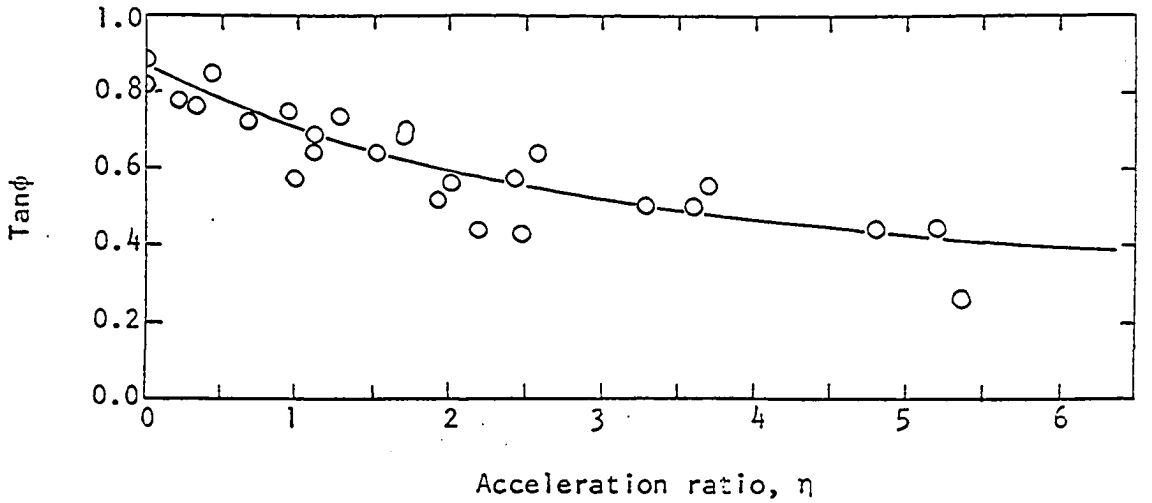

Figure 2. Relationship between the coefficient of internal friction of sand and the acceleration of vibrations. After Barkan, (1962)

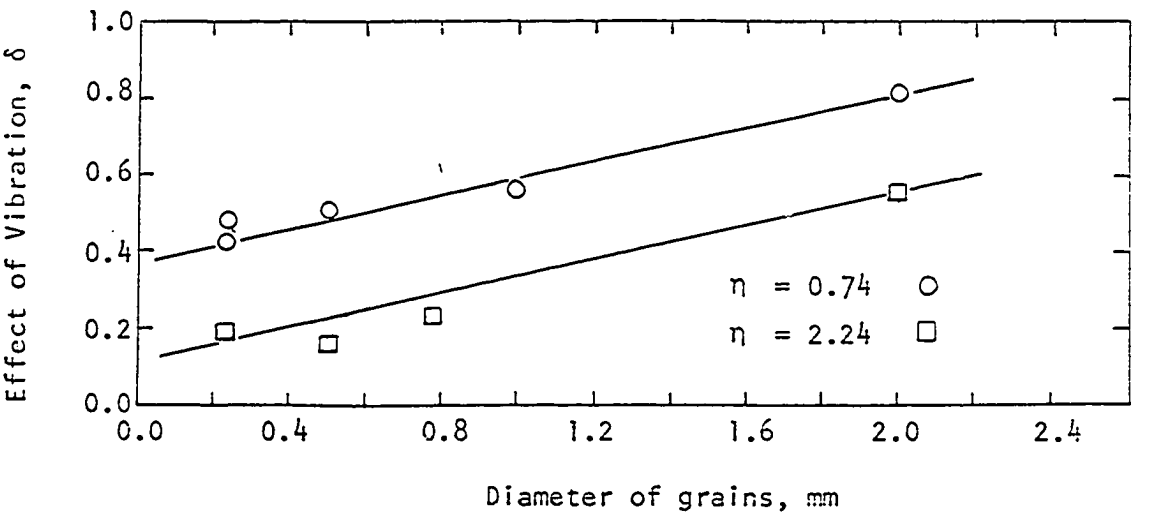

Figure 3. Relationship between the effect of vibrations and diameter of sand grains. After Barkan (1962).

Further investigations by Barkan showed that the reduction of internal friction by vibration was a function of the moisture content, with the reduction being about the same saturated sand as dry but less for intermediate moisture contents.

Mogami and Kubo (1953) conducted shear tests similar in principle to those reported by Barkan, except the shear apparatus was vibrated vertically and the normal load was applied by placing weights on the sample. They found that the shear strength of a sand and a loam diminished considerably with increasing vibration. With accelerations greater than twice that of gravity, the shear strength approached the shear strength of a static test with no normal load. They also concluded that the acceleration of the vibration rather than either the frequency or amplitude was the decisive factor in the "liquifaction" effects.

The results of Barkan and co-workers can not be directly compared with those of Mogami and Kubo since the loading conditions were vastly different. In the first case the normal load remained constant while the sample was vibrated thus the reduction of shear strength was due only to the vibration of the sample. In the latter case the strength reduction would be the combined effect of the sample vibration and an oscillating normal force, which would have an oscillating component due to the inertial forces on the weights used to apply the normal load.

Several investigators have investigated the effects of a vibrating normal stress on the shear strength of soils (Linger, 1963)(Mencl, 1957). This represents a completely different stress condition than those of the present investigation, which correspond more closely tc those of Barkan (1962) and associates; therefore, the results of these investigators will

not be reviewed here.

C. Vibrational Effects on Density

It has long been known that cohesionless soils could be densified by vibration. Among the first efforts to use vibration for compaction was in the development of vibratory equipment for tamping of ballast under railroad ties (Johnson, 1960). The advent of more and heavier wheel loads of airplanes and trucks created the necessity for better pavement bases. This necessity was met by improved design and construction procedures, including the development of vibratory compaction equipment. Along with this development, much research effort was directed at determining the factors involved in vibratory compaction.

As part of the investigation on the effect of vibration on soil properties by Barkan (1962) and associates, an investigation was made on the effect on soil density. Barkan reported the following: "Experiments show that the principal vibration parameter which determines the effect of vibration and shocks on the compaction of soils is the acceleration, or rather the inertial force, which acts on the soil particles during vibration." He further stated that the functional relationship between void ratio and acceleration was experimentally found to be the same for all soils. An experimental "vibratory consolidation curve" for sand is shown in figure 4 to illustrate this relationship. The data points shown represent a variety of frequencies and amplitudes.

By approximating this curve with an exponential curve, Barkan was able to formulate the following relationship between void ratio and the acceleration ratio for a soil densified from its loosest possible state.

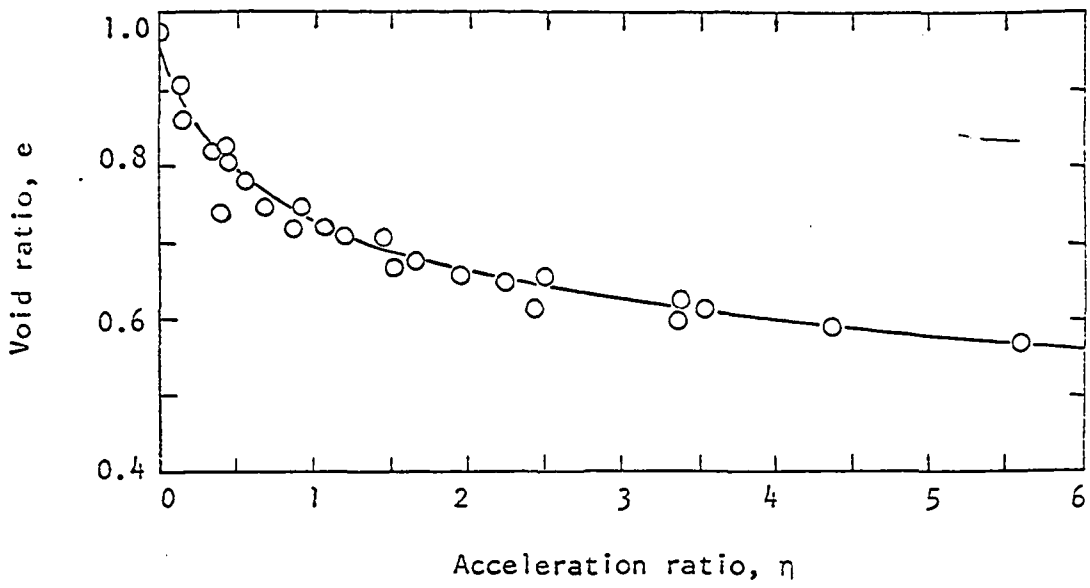

Figure 4. Vibratory consolidation curve of sand fill. After Barkan (1962)

$$e_v = e_{min} + (e_{max} - e_{min})\underline{e}^{-\alpha\eta} \qquad (9)$$

where: e_v = the void ratio of the soil after densification by acceleration η

e_{min} = the minimum limit value of the void ratio

e_{max} = the maximum limit value of the void ratio

α = a constant called the coefficient of vibratory compaction

$\underline{e}$ = the base of natural logarithms

This equation states that a loose sand vibrated at some acceleration, say η_o, will densify to some void ratio e_o. Barkan states that in order to further densify the sand, an acceleration greater than η_o must be applied. In the latter case η_o is termed the threshold of vibratory compaction. He also found that the threshold of vibratory compaction was a function of the applied normal stress, the larger the magnitude of this stress, the higher the threshold of vibratory compaction of the soil. Barkan attributed this effect of normal pressures on compaction to the fact that the forces of friction between particles of the soil increase with an increase of pressure on the soil, and thus vibrations can cause a smaller change in density.

In summary Barkan found that the threshold of vibratory compaction was dependent on both normal pressure and initial void ratio. In a further investigation he found that the coefficient of vibratory compaction, α, is also dependent on the moisture content of the soil.

In a more recent investigation Selig (1963) used a vertically vibrating container with normal pressures applied by weights to study the effects of vibration on the densification of dry silica sand. He concluded that

there was no correlation between density and any one of the vibrational parameters. However, a correlation was found between density and two of the parameters, acceleration and frequency. An increase in any one of the vibrational parameters produced an increase in density up to a limiting value above which density decreased. He further found that surcharge and increased depth of sand may assist or restrict increasing density caused by vibration. He explained this as follows: A certain amount of vibration is required to overcome the resistance to density change as a result of internal friction. This friction is increased by surcharge and added weight of sand. However, "overvibration" will loosen the particles, thus decreasing density.

There is a contradiction between Selig's conclusions and those of Barkan in that Barkan found that density was a function of only one vibrational parameter, acceleration; whereas Selig found two parameters were necessary to correlate his results. This contradiction could possibly be a result of different testing conditions; in Selig's investigation the normal pressure oscillated due to the inertial forces, thus normal pressure was also a function of the vibrational parameters. In Barkan's work the normal stresses were constant during vibration.

Viering (1961) also found that densification of granular soils was dependent on the acceleration and that vibrational densification decreased with increasing normal load. He also noted the existance of a threshold of vibratory compaction which he termed the "critical acceleration."

The mechanism of vibratory compaction was explained by Converse (1962) as follows: "The basic requirement for the compaction of soil is that the shearing resistance or friction between the particles of soil be reduced to

a point where the superimposed loads can press the particles closer together. This is true whether the soil is being compacted by static loads or by vibrating surface loads."

Winterkorn (1953) explained the mechanism of vibrodensification as one of loosening the contact of a particle with its neighbors for a sufficiently long period of time that the particle has time to assume, under the influence of gravity and normal pressure, positions of lower potential energy.

The mechanism given by Johnson and Sallberg (1960) is that particles in a granular system do not have equal contact pressures between particles. When a normal stress is applied some of the particles are forced into adjoining void spaces. If the normal pressure is released more relocations take place. Vibration consists of alternate loading and releasing the load. "Simply stated, adequate vibration meets those requirements of having sufficient force (dead weight plus dynamic force) acting through the required distance (amplitude) and giving sufficient time for movement of soil grains (frequency) to take place."

III. THEORETICAL CONSIDERATIONS

A. Mechanisms

In this section and in the section following on the effects of vibration, mechanisms are proposed to explain the actions which take place in a granular system subjected to shear forces or vibration or both. These proposed mechanisms are based on previously published studies and on observations made during the experimental portion of this investigation.

A particle in a granular system has a particular potential energy which is a function of its position, weight, and the external forces acting upon it. The system of particles has a potential energy which is the sum of the potential energies of each of the particles. The potential energy of the system has an upper and lower bound corresponding to the loosest stable state and the densest possible configuration respectively. The void ratio corresponding to the loosest possible state is e_{max}, and to the densest state, e_{min}.

Stability or equilibrium can occur at any void ratio between e_{max} and e_{min}. Moore (1963) defines equilibrium as follows: "A system is said to have attained a state of equilibrium when it shows no further tendency to change its properties with time."

A system at a void ratio greater than e_{min} is stable only because movement of particles to lower potential energy positions is prevented by the frictional and interlocking forces on the particles. These forces form an energy barrier over which the particle must pass in order to attain a lower energy state.

Figure 5 illustrates an energy barrier and three equilibrium states

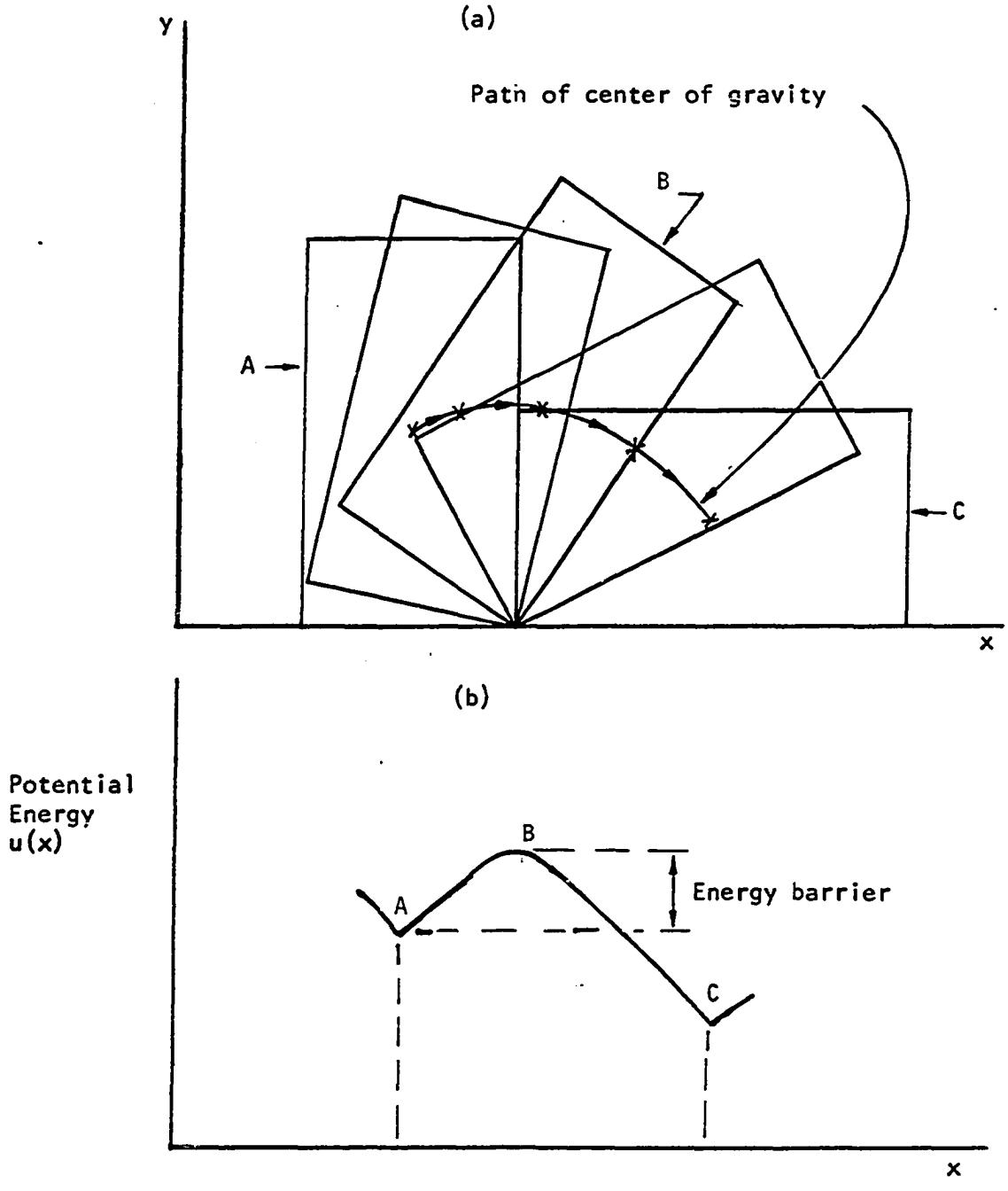

Figure 5. An illustration of mechanical equilibrium

for a simple mechanical model of a rectangular block resting on a table. In positions A and C the center of gravity of the block is lower than in any slightly rotated position; thus if the block is tilted slightly it will tend to return to its original position. The gravitational potential energy of the block in positions A and C is also at a minimum, and both positions represent stable equilibrium states. However, it is apparent that position C is more stable than position A since it is at a lower potential energy state.

Position B is also an equilibrium position, but it is a state of unstable equilibrium since stability in such a case can only exist in the complete absence of disturbing forces.

As the block is tipped from position A to B, the center of gravity rises, thus increasing the potential energy of the system. As the block rotates past position B, the potential energy decreases until it reaches the position C. Thus in order for the block to rotate from A to C, a sufficient force must be applied to push it over the energy maximum at B. The energy difference between A and B forms an energy barrier preventing the block from moving from position A to C on its own volition.

In a similar manner the particles in a granular system are prevented from moving to lower energy positions by an energy barrier caused by the frictional and interlocking forces acting on the particles.

In a random configuration of granular particles the contact pressures between particles are not equal; therefore, the energy barriers throughout the system are not equal. If a shear force is applied on a system at some void ratio greater than e_{min}, some particles will be given sufficient energy to overcome the energy barrier holding them in position. These

particles will then be free to move into lower energy positions and densification of the system occurs. Due to interlocking between particles some particles will be forced into higher energy positions by this same shear force, which results in dilatation of the system. These two processes may not occur simultaneously, and thus the system may contract before dilatation begins. If more dilatation occurs than densification, the system will expand until it reaches a state where densification equals dilatation -- in other words the amount of energy increase in the system due to particles moving over the energy barrier to higher energy states equals the energy decrease caused by other particles going over the energy barrier in the reverse direction. This condition corresponds to the critical void ratio condition as defined by Roscoe, Schofield and Wroth (1958). The CVR condition is thus an upper energy bound for a dilating system.

If the initial void ratio of the system were greater than that of the CVR condition, both dilatation and densification would still occur; however in this case a net decrease in potential energy would occur, accompanied by densification. The system would densify until the amount of dilatation equals the amount of densification, which again would be the CVR condition. Stable systems with void ratios greater than the CVR shall be referred to as states of "unstable equilibrium" since any disturbing force densifies the system.

Next let us consider a system at the CVR condition subjected to a shear force. In order for the particles on one side of a shear plane to move past those on the other side of the plane the energy barrier preventing movement must be overcome. The maximum resistance that any one

particle can offer to shear is the force necessary to push it to the maximum point on the energy barrier between its position and the next stable position. Summing up the resistance to shear of all of the particles involved at any instant of time gives the external shear force necessary to cause displacement. Thus the frictional resistance is a function of the energy barriers previously discussed. If the system were dilating, additional shear force would have to be applied to do work to dilate the system.

B. Vibrational Effects

If a system of granular particles is subjected to vibration, two separate actions occur. First the energy barrier is reduced. This reduction is caused by pulsating contact stress and possible separations between the particles. This action occurs even if the normal pressure applied to the system remains constant. This pulsating action between particles results in breaking of adhesional bonds, stress release and readjustment, which probably inhibits junction growth. The motion between particles would also reduce the frictional resistance due to microscopic interlocking. In this case the vibrational motion would aid one particle in climbing over the surface roughness of another.

The second vibrational action is the inertial forces of the particles. The maximum inertial force of a particle would be the mass of the particle multiplied by the maximum vibrational acceleration.

The following mechanism is proposed for vibrational densification: Consider a static system of particles, initially in equilibrium at its loosest possible state. The void ratio is e_{max} and is shown by point A in

figure 6. If the system of particles is vibrated at some acceleration, η_B. the energy barriers over which the particles must pass to move into lower energy positions is reduced by the mechanism proposed above. Simultaneously the particles are given an inertial force which gives a certain number of the particles potential to cross over the energy barrier into lower energy positions. Thus, densification proceeds until at some time when all of the particles capable of overcoming the energy barrier have done so, the system once again comes to a state of equilibrium. Such a state is shown by point B in figure 6, which represents the maximum energy state of the system for which equilibrium can occur for a given vibrational and loading condition. The void ratio at this state will be referred to as the "vibrational equilibrium void ratio" abbreviated by the initials EVR, and the corresponding vibrational and loading conditions will be referred to as the EVR condition.

If the vibration on the system is increased by an additional increment to η_D, the system again becomes unstable and further densification occurs until another EVR condition is reached shown by point D in figure 6. Thus the EVR is a function of η. This functional relationship is shown by the EVR line in figure 6.

If the acceleration is slowly reduced to zero from the EVR condition at D, no void ratio change will occur. As the acceleration is reduced, the energy barriers increase while the particle inertial forces decrease. Thus, the void ratio e_D is "locked" into the system, and the path followed in figure 6 is from D to A'.

If the vibration is slowly increased for the system initially at point A' in figure 6, no void ratio changes can take place at an acceleration

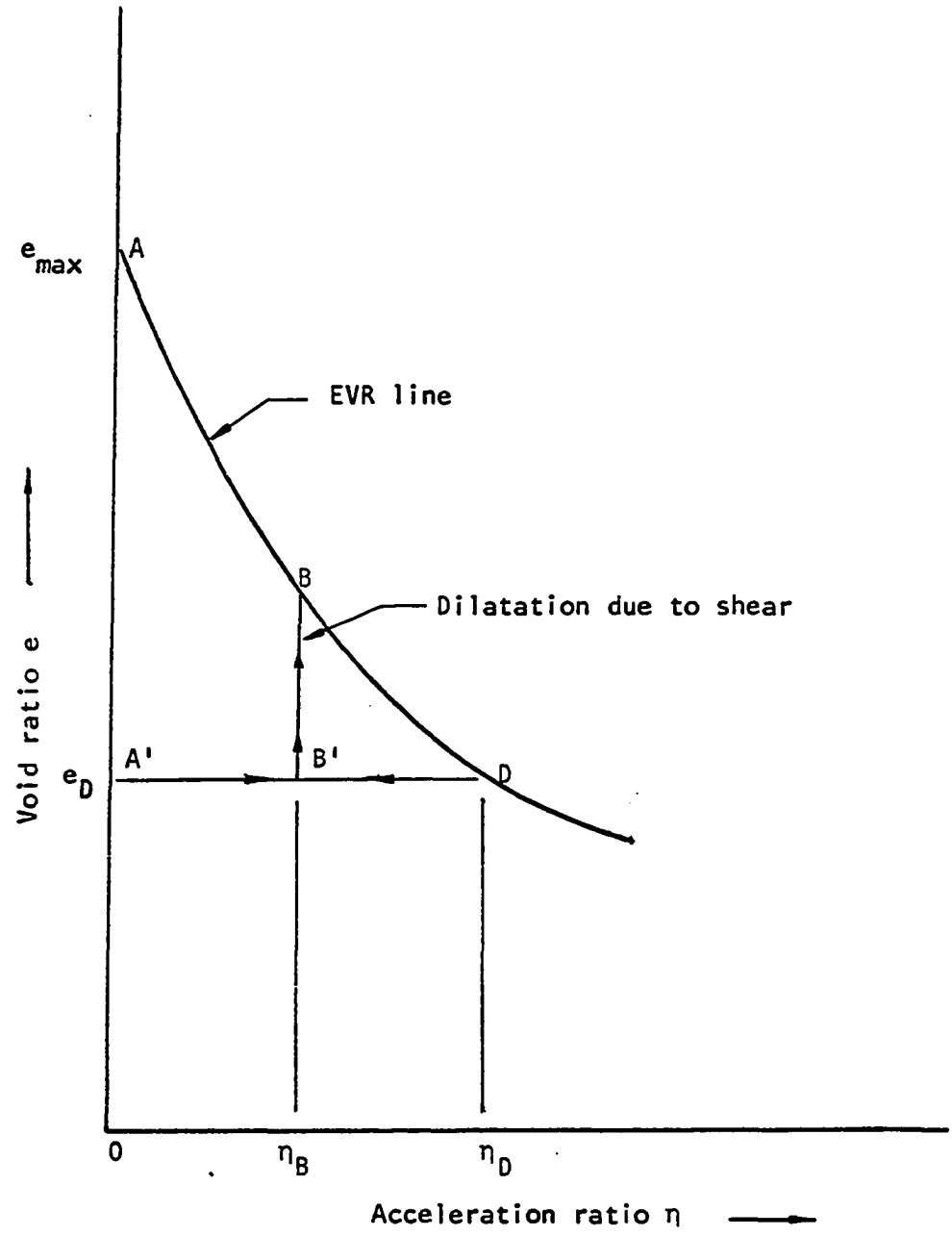

Figure 6. Relationship between void ratio and acceleration ratio

less than η_D. This is because all of the particles which were able to move into lower energy positions at an acceleration η_D had done so previously and thus no relocations occur in reaccelerating the system. If the acceleration is increased to η_D the system is again in the EVR condition and any further increase of acceleration will cause further densification. This phenomenon was observed and referred to as the "threshold of vibratory compaction" by Barkan (1962) and as the "critical acceleration" by Viering (1961). However in this thesis it shall be referred to as the EVR condition.

Next consider a system in an EVR condition subjected to a shearing force. As shear distortion occurs in the system, interlocking causes some particles to move into higher energy configurations, thus tending to dilate the system. However, the higher energy configurations are unstable due to the vibrational effects, and these particles are able to move into other lower energy positions. Therefore it would be expected that very little volume change would occur during shear distortion of a system in the EVR condition. This also corresponds to the definition of the CVR condition, thus making the EVR and the CVR equivalent.

The force necessary to shear the system should be less than the force necessary to shear it in a static condition at the CVR if the energy barrier preventing movement of particles is smaller than for the static case. It was previously postulated that the frictional resistance was a function of the energy barriers. Therefore, frictional resistance decreases with increased acceleration.

Next consider a system with a void ratio less than the EVR void ratio, say a void ratio of e_D and an acceleration of η_B in figure 6. If the

system is then sheared, dilatation will occur since particles in this case can be moved into higher energy configurations without the vibrational effects being able to totally redensify the system. The state of the system thus moves along a path from B' to B in figure 6. Dilatation can not proceed past the EVR condition since at that point densification would take place at the same rate as dilatation, and the CVR condition would be reached. This means that the interlocking component of the shear strength as well as the frictional component is reduced by vibration because the amount of dilatation the system undergoes to reach the maximum stable void ratio is less.

C. Analysis[1]

1. Shear strength

Up to this point it has been proposed that the frictional resistance is a function of the energy barriers in a granular system. These energy barriers are reduced by vibration, thus reducing the frictional resistance. The energy barriers are a function of the physical properties of the particles, the normal pressure and the vibrational parameters.

At the EVR condition where dilatation is essentially zero, the coefficient of friction can be expressed in the following functional form:

$$\tan\phi_v = f(\omega, a, g, \sigma_{11}, d, E, M) \qquad (10)$$

$\tan\phi_v$ = the coefficient of internal friction at the EVR condition; dimensionless.

ω = the frequency of vibration; dimensionally T^{-1}

[1] A list of symbols used is given in appendix A.

a = the amplitude of vibration; dimensionally L

g = the acceleration of gravity; dimensionally LT^{-2}

σ_n = the normal pressure; dimensionally FL^{-2}

d = the particle diameter; dimensionally L

E = the modulus of elasticity of the particles; dimensionally FL^{-2}

M = other properties of the particles

The intent of this investigation was to study the effect of vibration on a granular system. Therefore, only the vibrational parameters and the normal pressure, which may influence the effect of the vibration on the system, shall be analyzed. All of the properties of the particles are thus grouped into one factor M except for d and E, which are convenient to use in the analyses. The term M is a constant for any one material and is not affected by vibration.

By the methods of dimensional analysis (Murphy, 1950) the terms in equation 10 can be combined into dimensionless pi-terms. In terms of these pi-terms equation 10 becomes:

$$\tan\phi_v = f(\eta,\ a/d.\ E/\sigma_n,\ \pi_M) \qquad (11)$$

where $\eta = \omega^2 a/g$ and π_M represents pi-terms involving the parameters grouped into the term M.

A prediction equation could be formulated for $\tan\phi_v$ by experimentally investigating the relationships between the pi-terms. However, by making a few pertinent assumptions the form of the relationship can be obtained. Then by experimental investigation the relationship and assumptions can be verified and parameters of the relationship evaluated.

When the acceleration ratio is zero, the vibrational parameters have no effect and $\tan\phi_v = \tan\phi_{st}$. As η becomes large, $\tan\phi_v$ approaches some limiting minimum value, $\tan\phi_{min}$, greater than zero. $\tan\phi_{min}$ is greater than zero since at any time there must be sufficient interparticle contact, and thus adhesional bonding and microscopic interlocking, to transfer the applied normal stress through the system. $\tan\phi_{st}$ and $\tan\phi_{min}$ are limiting values which may depend on E/σ_n but are independent of η and a/d.

The first necessary assumption is that

$$\tan\phi_v = f(\beta\eta) \tag{12}$$

where $\beta = F(a/d,\ E/\sigma_n,\ \pi_M)$

The second assumption is that at any EVR condition, the amount of reduction of $\tan\phi_v$ caused by an incremental increase in η is proportional to the total amount of decrease possible at that state, $(\tan\phi_v - \tan\phi_{min})$. Written mathematically

$$\frac{d\ \tan\phi_v}{d\eta} = -\beta(\tan\phi_v - \tan\phi_{min}) \tag{13}$$

Integrating yields

$$\ell n(\tan\phi_v - \tan\phi_{min}) - \ell n\ C = -\beta\eta \tag{14}$$

where $\ell n\ C$ is a constant of integration. The antilogarithm of equation 14 is:

$$(\tan\phi_v - \tan\phi_{min}) = C\ e^{-\beta\eta} \tag{15}$$

The constant C can be evaluated by applying the conditions for $\eta = 0$.

$$(\tan\phi_v - \tan\phi_{min})]_{\eta=0} = (\tan\phi_{st} - \tan\phi_{min}) = C \qquad (16)$$

The final form of the functional relationship is thus:

$$\tan\phi_v = \tan\phi_{min} + (\tan\phi_{st} - \tan\phi_{min})e^{-\beta\eta} \qquad (17)$$

where $\beta = F(a/d, E/\sigma_n, \pi_M)$ and shall be evaluated experimentally. The exponent β will be referred to as the coefficient of shear strength reduction.

Equation 17 is the same as equation 7 empirically determined by Barkan (1962).

The functional relationship between tan ϕ and η for a system initially at a void ratio less than the EVR is more complex than at the EVR condition due to the dilatation factor. In this case two equations are necessary. The first equation is valid for $\eta \leq \eta_{EVR}$ where η_{EVR} is the acceleration at the EVR condition. This is represented by curve a in figure 7. The second equation is equation 17 which is valid for $\eta \geq \eta_{EVR}$ and is represented by curve b in figure 7.

In this case the equation of curve a shall be assumed to be of the form

$$\tan\phi = A + (\tan\phi_{st} - A)e^{-\beta_2\eta} \qquad (18)$$

This equation is valid only for $\eta \leq \eta_{EVR}$. The constant A has no physical significance.

By measuring volume changes during shear it may be possible to separate equation 18 into frictional and dilatational components by use of equation 5.

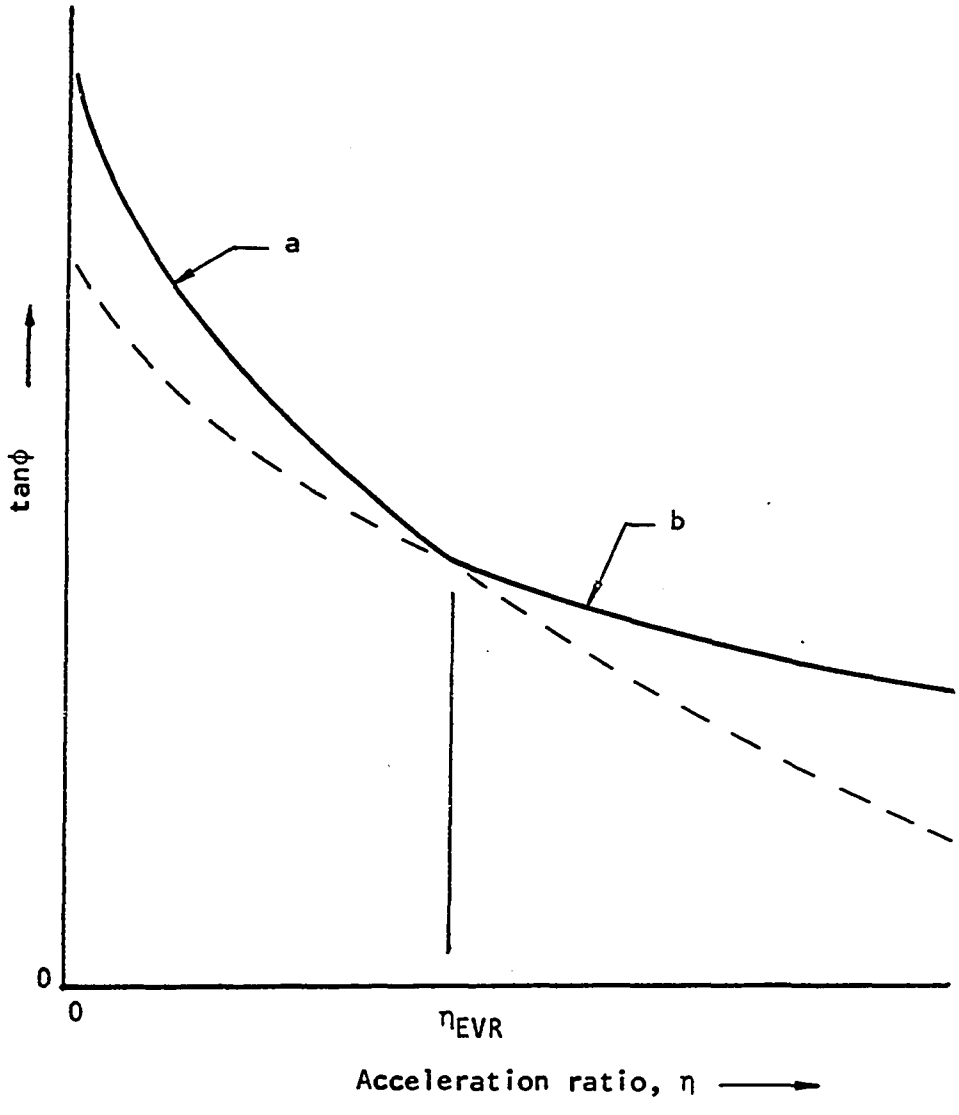

Figure 7. The relationship of tanϕ to η

a. $\tan\phi = A + (\tan\phi_{st} - A)e^{-\beta_2\eta}$

b. $\tan\phi_v = \tan\phi_{min} + (\tan\phi_{st} - \tan\phi_{min})e^{-\beta\eta}$

2. Densification

It was proposed that vibrational densification occurs by a process of particles being able to surmount the energy barrier holding them in place and move into lower energy positions. This process can only occur as long as there are lower energy positions available for particles to move into. As the system densifies, the availability of lower energy positions decreases until at e_{min} there is no further possibility for densification by vibratory action.

Making the assumption that the change in void ratio caused by an incremental increase in acceleration is proportional to $(e_v - e_{min})$ for a system in the EVR condition, the following mathematical equation can be written.

$$\frac{de_v}{d\eta} = -\alpha(e_v - e_{min}) \tag{19}$$

Integrating and taking the anti-logarithm

$$\frac{\int de_v}{(e_v - e_{min})} = -\int_0^{\eta} \alpha d\eta$$

$$\ell n(e_v - e_{min}) - \ell n\ D = -\alpha\eta \tag{20}$$

where $\ell n\ D$ is a constant of integration

$$(e_v - e_{min}) = D\ \underline{e}^{-\alpha\eta} \tag{21}$$

For $\eta = 0$

$$(e_v - e_{min})]_{\eta=0} = (e_{max} - e_{min}) = D$$

Thus the final form of the equation is

$$e_v = e_{min} + (e_{max} - e_{min})\underline{e}^{-\alpha\eta} \qquad (22)$$

The second assumption is that $\alpha = G(a/d, E/\sigma_n, \pi_M)$. This equation is the same as equation 9 which was derived experimentally by Barkan (1962), the coefficient α being termed the coefficient of vibratory compaction.

For a system initially at a void ratio less than the EVR, no change in void ratio occurs as the acceleration is increased until $\eta = \eta_{EVR}$. Equation 22 is then valid for any further increase in η.

IV. TEST APPARATUS AND PROCEDURE

A. Requirements

In order to experimentally investigate the validity of the theory developed in the previous chapter, a testing method and apparatus were developed. Since the purpose of the investigation was to investigate the effect of vibration on a granular system, it was necessary that the vibrational parameters be varied independently of any other parameters of the system. The physical condition to be simulated in the tests was that of a confined mass of soil which could be vibrated and sheared while holding the normal stress constant. Other requirements were that the normal stress, shear stress and void ratio be either known or be determinable at any stage of the test.

At the present time there are two common methods for laboratory shear testing of soils, the triaxial compression test and the direct shear test. There are suggested testing methods listed for both of these tests by the American Society for Testing and Materials (1964). Although there are a number of advantages in using a triaxial compression test (Lamb, 1951), such as being able to obtain a stress-strain diagram and knowing the stress conditions on any plane at any time during the test, the problem of the inertial force on an unsupported column of soil was formidable. Therefore, the simpler direct shear apparatus was considered.

Although the direct shear test has the disadvantages of only being able to determine the principal stresses on the failure plane at the time of failure, and not being able to determine a stress-strain diagram, there are several important advantages in the direct shear test. Beside

simplicity there was the ease with which volume changes could be measured, which was very important in this investigation. However the determining factor in the decision to use the direct shear tests was that the soil is confined in a shear box, thus eliminating the problem of inertial forces on a laterally unsupported column of soil.

B. Apparatus and Materials

It was necessary to construct a special testing apparatus to meet the necessary requirements of the investigation. This apparatus was then mounted on a commercially made shaker table.[1] A schematic drawing of the direct shear device is shown in figure 8. The upper ring of the shear box was rigidly clamped to the vertical supporting rods, and the lower ring was supported on ball bearings riding in a track, thus allowing the lower ring to be displaced during a test. The normal load was applied by a low-friction air cylinder. The shear load was applied by a wire pulling on the lower ring; this allowed the worm gear drive mechanism to be separate from the table.

Since it would be impossible to read dials during vibration, measurements of vertical and horizontal displacements were made by cantilevers (6-inch stainless steel rules) equipped with SR-4 electrical resistance strain gages. The cantilevers were rigidly attached to the table and were deflected by the displacements. The shear load was measured from a proving ring also equipped with SR-4 strain gages. Both vertical and horizontal displacements, and the shear load were recorded on a constant-speed single

---

[1] All American Fatigue Testing Machine model 25-HA-D, All American Tool and Mfg. Company, Skokie, Ill.

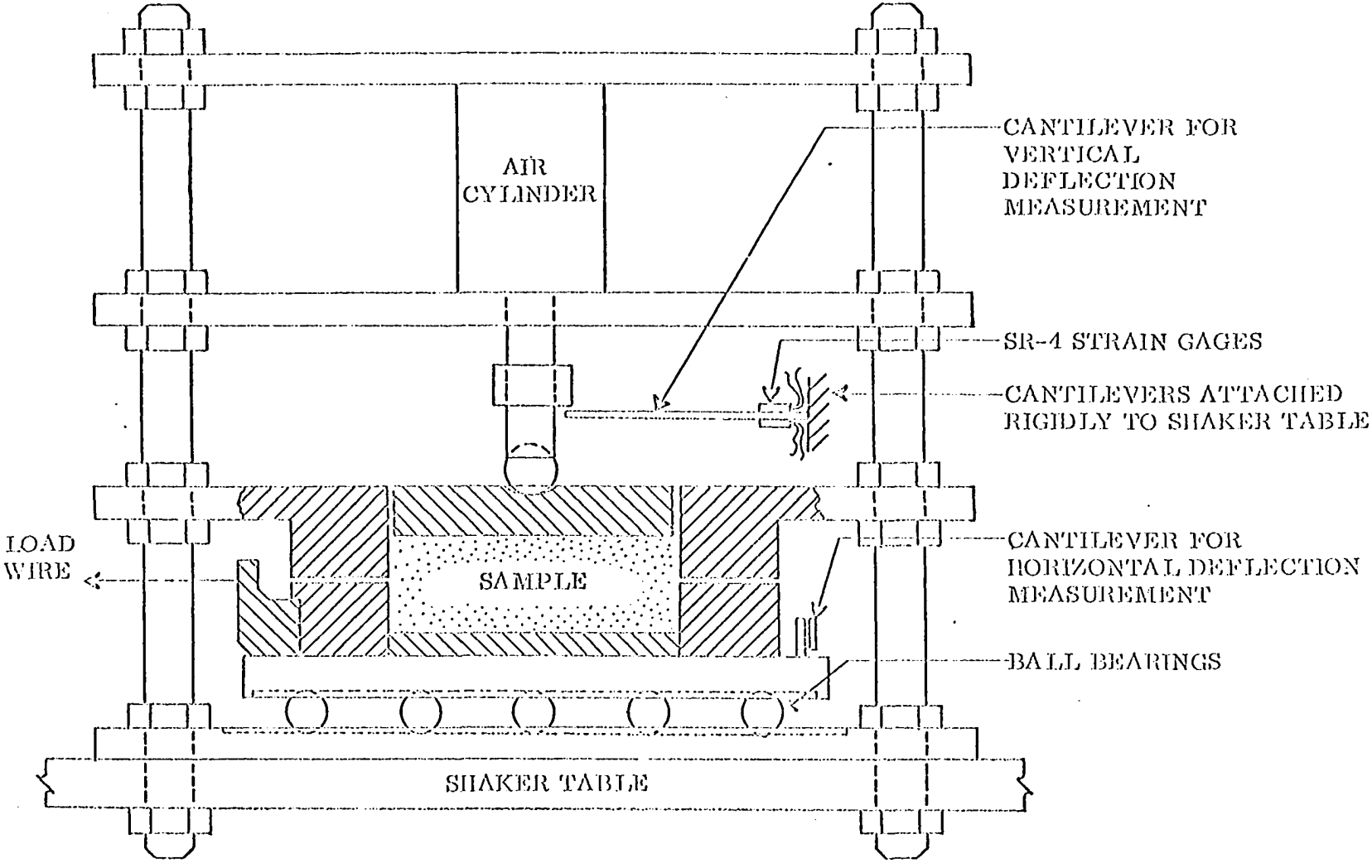

Figure 8. Direct shear apparatus

pen strip chart recorder[1] with the aid of a manual switching apparatus. The normal load was computed from the air pressure supplied through a commercial air regulator[2] to the air cylinder.

The shear apparatus was oriented on the table in such a manner that the shear displacement was horizontal and at right angles to the direction of table motion. The normal load was applied vertically. With this orientation the effect of the vibration on the mechanical components of the apparatus was minimal, providing the wire applying the shear load was long enough to make the change in length between the shear device and the proving ring negligible. This change in length was due to the table motion being perpendicular to the line of action of the wire. In the test setup the length of the wire was over sixteen inches, whereas the maximum amplitude of vibration was only 0.075 inches.

The shaker table was of the direct-drive type with a horizontal-one-direction table motion. A check of the time-displacement characteristics of the table motion with the aid of an oscilloscope showed the motion to be sinusoidal. Both frequency and amplitude were adjustable, the amplitude being variable from 0 to 0.075 inches and the frequency being variable from 10 to 60 cycles per second.

Figure 9 is a photograph of the general layout of equipment. A close-up photograph of the shear apparatus is shown in figure 10.

The shear box was 2.528 inches in diameter and the height of the sample was between 0.6 and 0.7 inches, depending on the void ratio. The load cap and the base plate were equipped with ridges similar to those

[1]Sargent recorder model MR, E. H. Sargent and Co., Chicago, Ill.

[2]Air Regulator model KWPR 125, Karol Warner, Inc., Highland Park, N.J.

Figure 9. General layout of equipment.

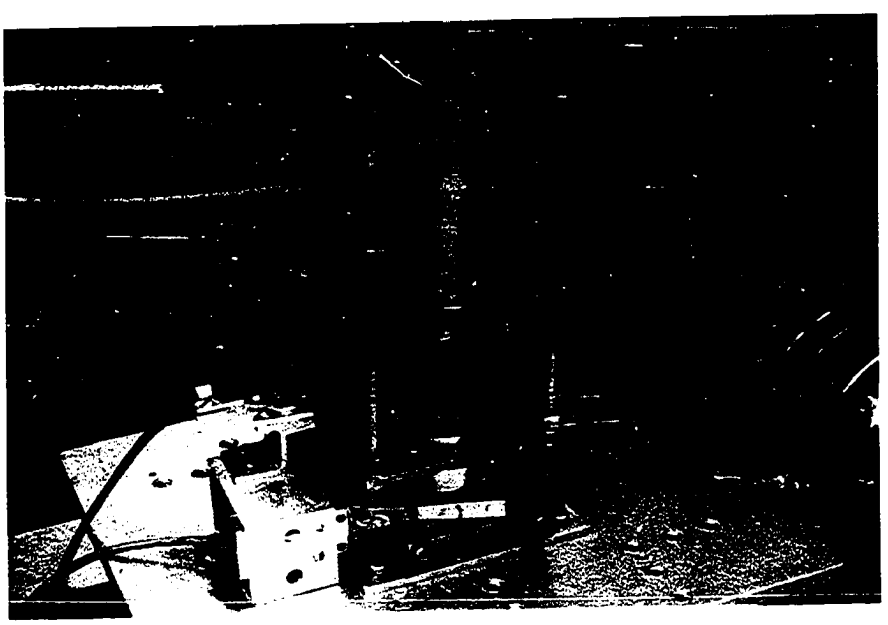

Figure 10. Shear apparatus

found on the caps of commercially made direct shear devices. The maximum possible shear displacement was 0.4 inch.

One of the major difficulties encountered during testing was binding between the load cap and the upper ring. This difficulty was solved by placing a felt liner between the load cap and upper ring. Another difficulty was intrusion of particles between the rings during shear displacement; this was solved by making the clearance between the rings smaller than the diameter of the smallest particle.

The materials used in the tests were standard Ottawa sand passing the No. 20 and retained on the No. 30 sieve, and the following sizes of steel balls: 1/16, 3/32, 1/8, and 5/32 inch. The sand was prepared for testing by oven-drying it for 24 hours and then cooling in the laboratory atmosphere just prior to testing. The steel balls were cleaned in acetone and air-dried prior to testing. Only one size of balls was placed in the shear apparatus for any one test.

C. Procedure

A preweighed quantity of the material to be tested was poured into the shear box in as loose a condition as possible. The sample was then carefully leveled with a rod, disturbing the sample as little as possible. The weight of the sample placed in the shear box was calculated to give an equivalent height of solids of 0.400 inch.

The void ratio is defined as the ratio of the volume of the void space to the volume of the solids. Since the cross-sectional area of the sample remained constant at all times, the void ratio was calculated from the following relation:

$$e = \frac{H-H_s}{H_s} \qquad (23)$$

H = the height of the sample

H_s = the equivalent height of solids

From equation 23 it is seen that the void ratio is a linear function of the sample height; therefore, the vertical transducer was calibrated to read out directly in terms of void ratio.

After the sample was leveled, the load cap was carefully placed on the sample, and the piston of the air cylinder was lowered to bear on the load cap. The normal load for the test was then applied by introducing the required air pressure into the cylinder. The vibrator was then started and the sample densified by vibration.

If the test was to be an EVR condition shear test, the amplitude and frequency of the test were set on the vibrator and the sample was allowed to vibrate for three minutes. Three minutes is considered an adequate time for complete densification of small samples of granular materials (Major, 1962)(Spanovich, 1964). If the shear test was to be conducted at a void ratio less than the EVR, the sample was compacted at a greater acceleration ratio until the desired void ratio was attained, then the acceleration ratio was reduced to that of the test. If the test was only to determine the void ratio at the EVR condition without running the corresponding shear test, the following procedure was followed: The sample was placed in the shear box as before, the normal load of the test applied and the desired amplitude was set on the vibrator. The sample was then vibrated for three minutes at a low frequency. Since the frequency could be changed while the table was in motion, the frequency was then increased in

increments, allowing the sample to vibrate for three minutes at each frequency. Thus a complete EVR curve was obtained from one sample.

After compaction, the sample was sheared while subjected to vibration at the desired amplitude and frequency. Static shear tests were also made with the same shear device as part of the investigation. During shear, the shear load, the horizontal displacement, and the vertical displacement, read out in terms of void ratio, were recorded on the chart recorder by alternately switching from one transducer to another.

Since all the materials used in this investigation were cohesionless, the coefficient of internal friction for the test was computed from the formula:

$$\tan\phi = S_m/N \qquad (24)$$

where S_m = the maximum shear load

N = the normal load of the test.

V. PRESENTATION AND ANALYSIS OF RESULTS[1]

An experimental investigation was conducted to test the theory proposed in the chapter on theoretical considerations. Shear tests as well as densification tests were made at the EVR condition and at void ratios less than the EVR. A summary of the results of the tests referred to and used in the experimental analysis is tabulated in appendix B.

A. Vibrational Effects on Density

The results of a series of tests made on 1/16 inch steel balls to determine the effect of the pi-term (a/d), vibrational amplitude divided by the particle diameter, on the EVR are shown in figure 11. This was accomplished by varying a and ω while holding η and the pi-term (E/σ_n) constant. These results show that the EVR is independent of (a/d) and therefore η is the only vibrational parameter on which the EVR is dependent.

EVR values obtained by varying η for several different values of σ_n are shown in figure 12 for 1/16 inch steel balls and in figure 13 for Ottawa sand. Figure 14 shows the same results for several ball sizes at a normal pressure of 20 psi.

A non-linear regression was performed to fit the data of the tests shown in figures 12, 13 and 14 to equation 22 and to determine the best estimates of the parameters e_{max}, e_{min} and α. Since only the first portion of the total e_v versus η curve was experimentally determined, there was no direct way of obtaining an estimate of e_{min}. Therefore, the parameter e_{min} was replaced by e_∞ where e_∞ was determined by extrapolating the e_v versus η curve to a value of η approaching infinity.

[1] A list of the symbols used is given in appendix A.

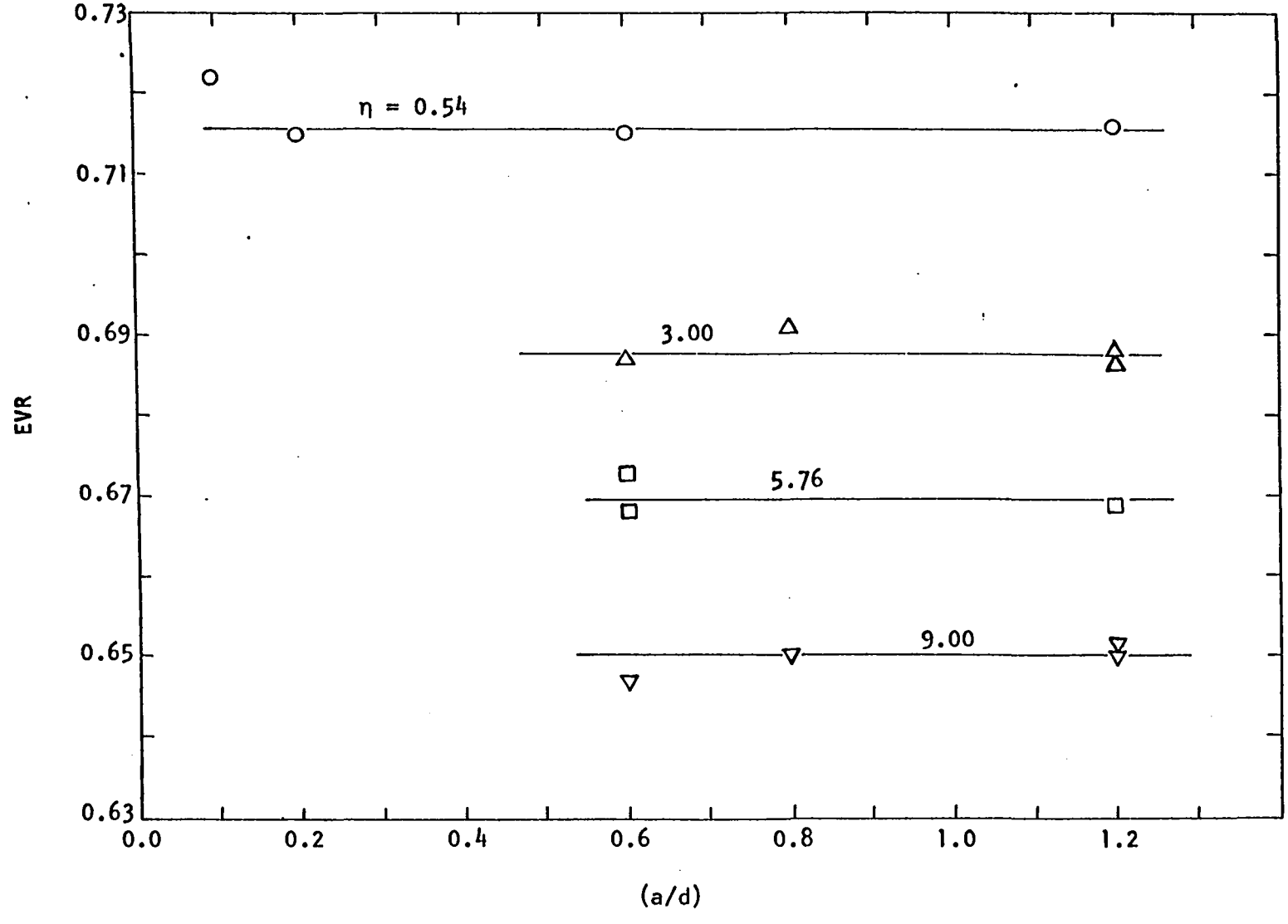

Figure 11. Vibratory equilibrium void ratios for various (a/d) ratios for 1/16 inch steel balls at a 10 psi normal pressure

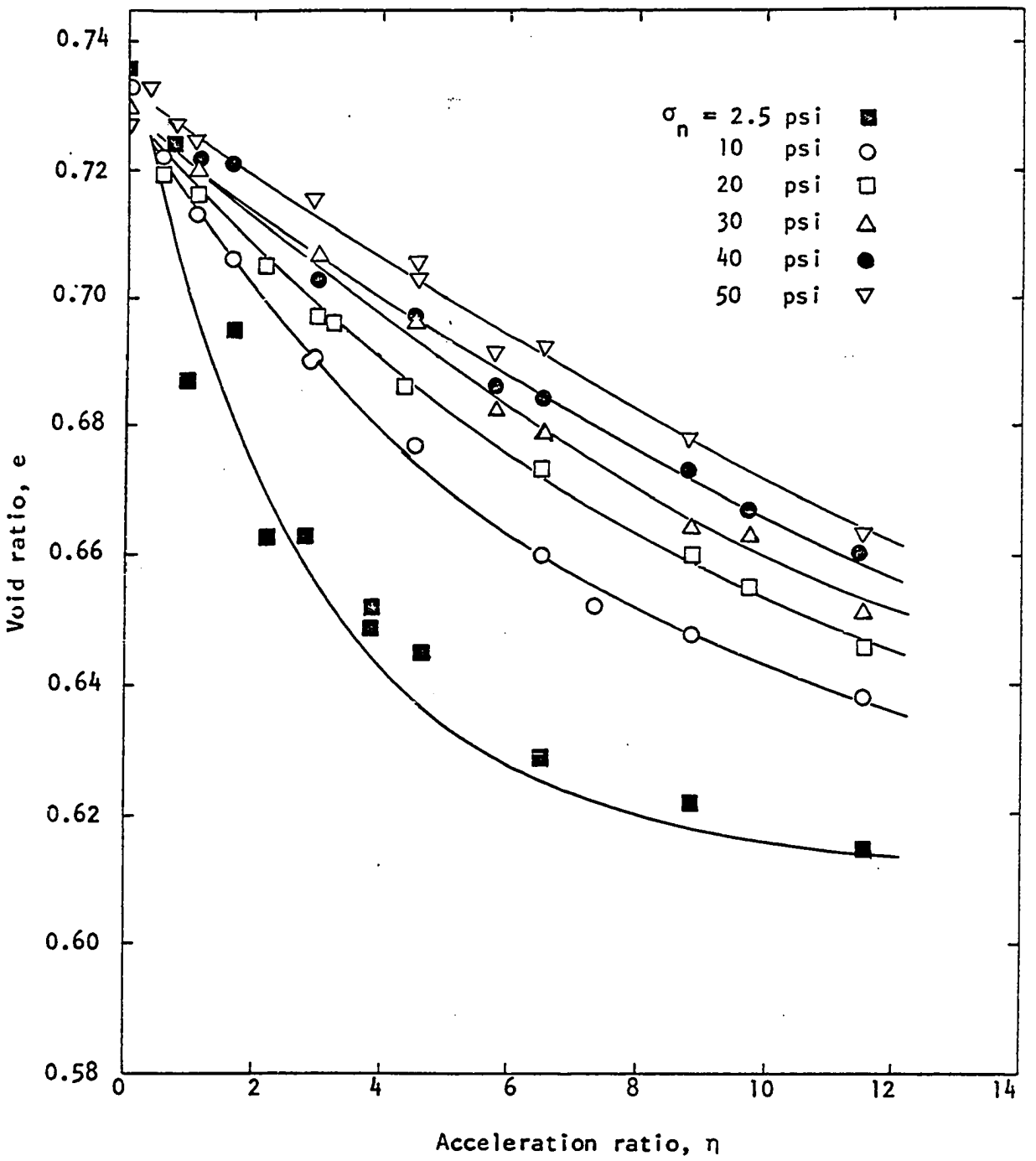

Figure 12. EVR curves for 1/16 inch steel balls

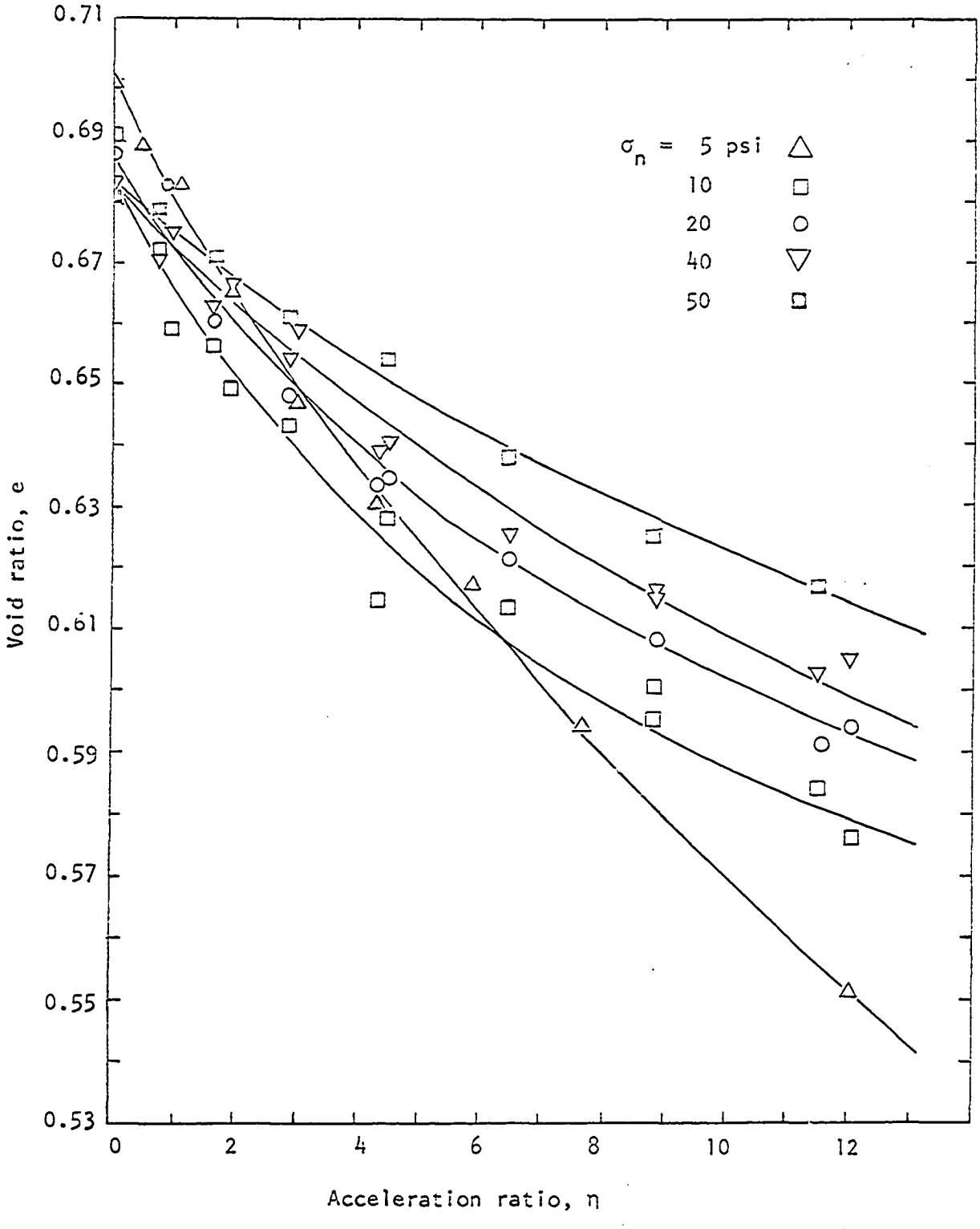

Figure 13. EVR curves for Ottawa sand

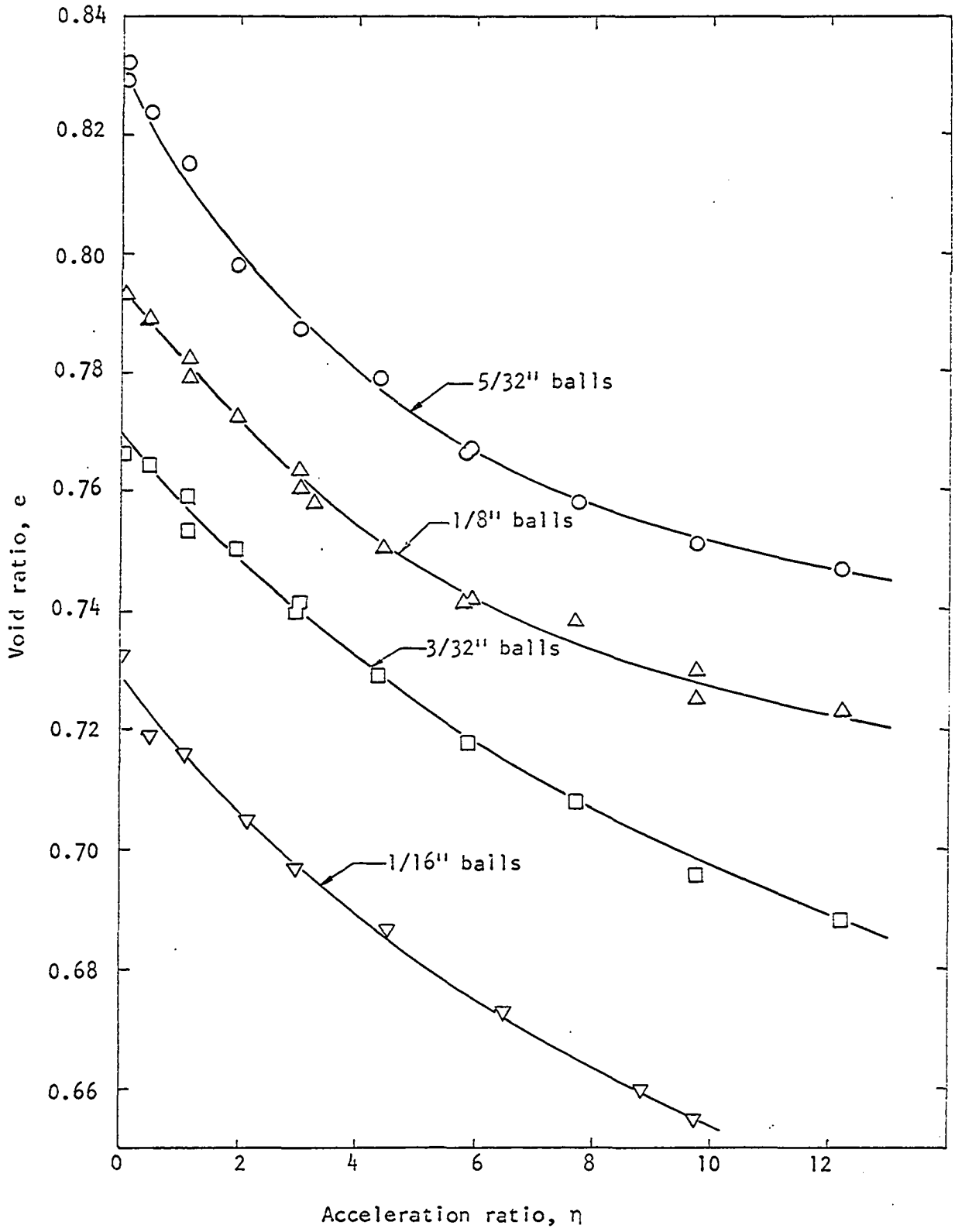

Figure 14. EVR curves for steel balls at 20 psi normal pressure

These non-linear regressions were performed by an electronic computer using "Hartley's modified Gauss-Newton method for fitting of non-linear regression functions by least squares" (Atkinson, 1966) (Hartley, 1961). Equation 22 was then written as follows:

$$z = \ln \left(\frac{e_v - e_\infty}{e_{max} - e_\infty} \right) = -\alpha\eta \qquad (22a)$$

and a linear regression computed between z and η. From the linear regression the correlation coefficient r was determined. The results of the computer analysis are tabulated in table 1.

The curves drawn in figures 12, 13 and 14 are the theoretical curves determined by substituting the computed estimates of the parameters into equation 22.

For a perfect positive correlation the value of r is one, whereas a value of zero indicates no correlation. Thus the correlation between the theoretically predicted values and the experimental values was very good.

In figure 15 the values of the coefficient of vibratory compaction for 1/16 inch balls and sand are plotted against the reciprocal of the normal pressure. The reciprocal of the normal pressure was used since multiplying this by the modulus of elasticity of the particles gives the dimensionless pi-term (E/σ_n). From the curves in figure 15 it appeared probable that α and σ_n could be related by an empirical relationship of the following form:

$$\alpha = \left(\frac{1}{\sigma_n} - 0.015 \right)^p \qquad (26)$$

for σ_n in psi. This was substantiated by plotting $\ln \alpha$ against $\ln \left(\frac{1}{\sigma_n} - 0.015 \right)$ in figure 17. Equation 26 fit the data for 1/16 inch

Table 1. Estimates of e_m, e_∞ and α, and the correlation coefficient r

Material	σ_n, psi	e_{max}	e_∞	α	r
1/16" balls	2.5	0.739	0.613	0.375	0.988
1/16" balls	10.0	.733	.617	.154	.998
1/16" balls	20.0	.729	.607	.0966	.999
1/16" balls	30.0	.731	.588	.0683	.997
1/16" balls	40.0	.729	.565	.0487	.997
1/16" balls	50.0	.732	.507	.0310	.997
3/32" balls	20.0	.767	.623	.0957	.984
1/8" balls	20.0	.794	.710	.157	.991
5/32" balls	20.0	.830	.739	.208	.998
sand	5.0	.698	.418	.0610	.999
sand	10.0	.683	.557	.141	.989
sand	20.0	.687	.565	.120	.990
sand	40.0	.683	.540	.0732	.988
sand	50.0	.683	.557	.0656	.998

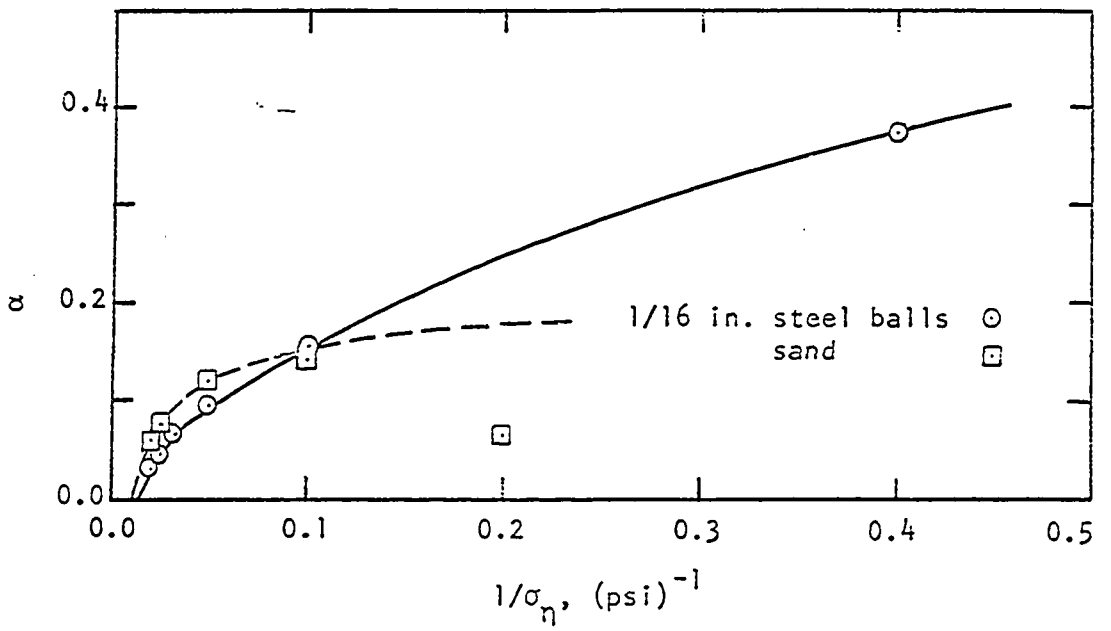

Figure 15. The relationship between α and normal pressure

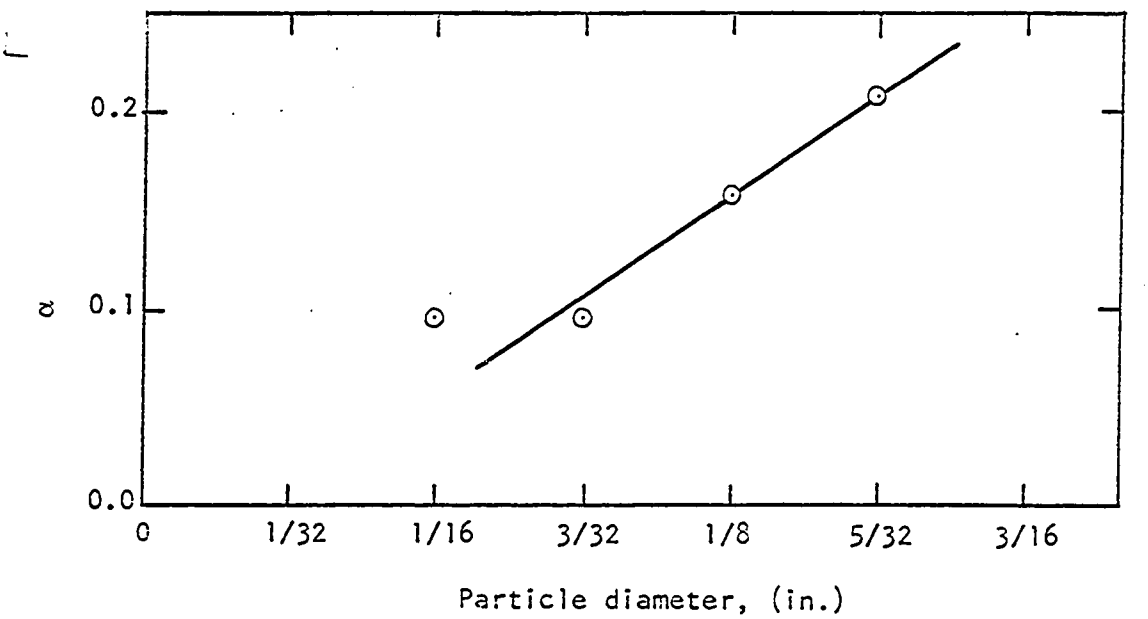

Figure 16. The relationship between α and particle size for steel balls

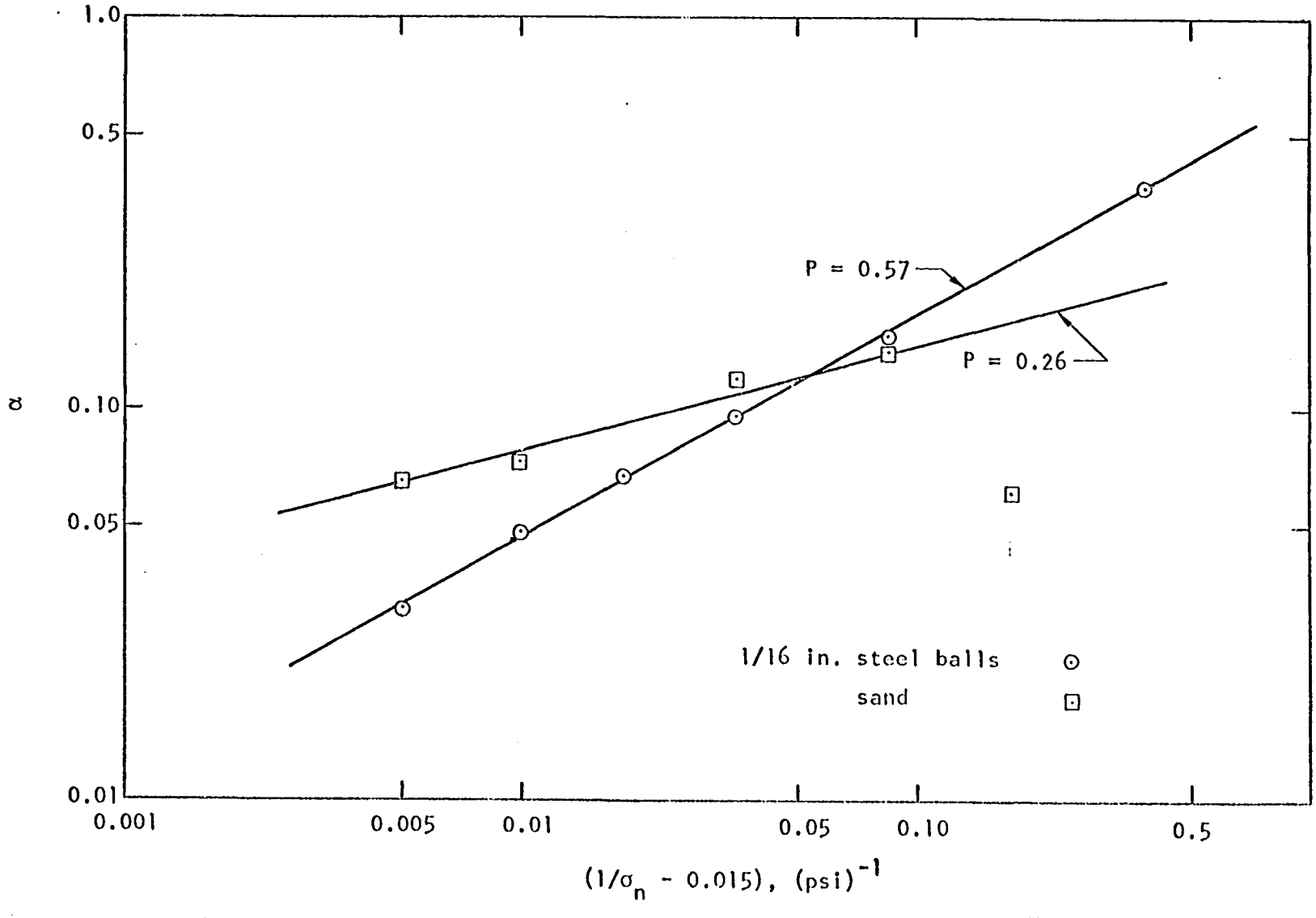

Figure 17. A logarithmic plot of the equation $\alpha = (1/\sigma_n - 0.15)^m$ for σ_n in psi

steel balls very well, giving a value for p of 0.57. For a p value of 0.26 the equation fit the data for the sand fairly well except for the data point at 5 psi normal pressure. This point appears to be of questionable validity. The estimated value of e_∞ for this same normal pressure appears to be in disagreement with the other values of e_∞ determined for sand, as shown in figure 18.

Figure 16 shows the relationship found between α and particle size for steel balls. The data could be fit rather well by a straight line with the exception of the point for the 1/16 inch ball size. The 1/16 inch balls had been used in numerous tests whereas the other balls had been used relatively little when the tests in question were conducted. It was noted during testing that the test results were very sensitive to surface condition; hence the cleaning with acetone. The reason for this one point appearing to be in disagreement may have been due to a difference in surface condition.

Figure 18 shows the estimates of e_{max} and e_∞ plotted against normal pressure for sand and for 1/16 inch steel balls. The parameter e_∞ was estimated from the regression by extrapolating the best fitting curve to a value of η approaching infinity. Therefore the computed value of e_∞ is valid as a parameter in equation 22 for the range of acceleration ratios tested, but it is not valid as an estimate for the minimum void ratio e_{min}.

It was found that the parameters e_{max} and e_∞ increase with ball size. This was thought to be due only to the edge effects of the shear box, since the void ratio for any particular packing of balls is independent of the ball size.

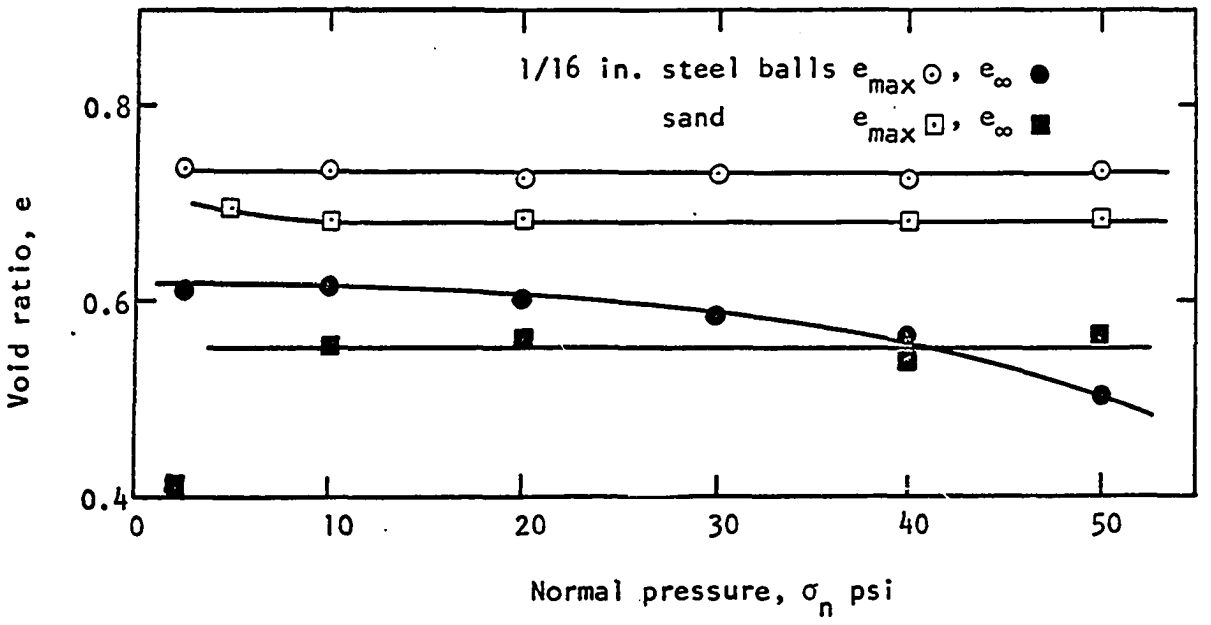

Figure 18. Estimates of the parameters e_{max} and e_∞ versus normal pressure

B. Vibrational Effects on Shear Strength

The results of a series of tests to determine the effect of the pi-term (a/d) on $\tan\phi_v$ for 1/16 inch balls are shown in figure 19, and indicate that $\tan\phi_v$ was independent of (a/d). Thus η is the only vibrational parameter affecting $\tan\phi_v$.

Data from shear tests at the EVR condition for various normal pressures are shown in figures 20 thru 23 for 1/16 inch steel balls and in figure 24 for Ottawa sand. Figure 25 shows the relationship between $\tan\phi_v$ and η for three sizes of steel balls at 20 psi normal pressure.

The data for these series of tests were analyzed by the same computer procedure as the densification tests previously discussed, except the non-linear regression model in this case was equation 17 rather than equation 22. A tabulation of the parameters $\tan\phi_{st}$, $\tan\phi_\infty$ and β is given in table 2 where the parameter $\tan\phi_\infty$ is an estimate of $\tan\phi_{min}$ as η approaches infinity.

The non-linear regression converged to nonsensical values for the sand subjected to a 10 psi normal pressure. Therefore, a value of 0.400 was assumed for $\tan\phi_\infty$ and the regression was computed using this value to obtain the other two parameter estimates and the correlation coefficient.

The curves drawn in figures 20 thru 25 are the theoretical curves determined by substituting the computed parameters, tabulated in table 2, into equation 17. The values of the correlation coefficients tabulated indicates a very good fit between the theoretical relationship and the experimental data.

In figure 26 the estimates of β are plotted against the reciprocal of the normal pressure for both sand and 1/16 inch steel balls. From these

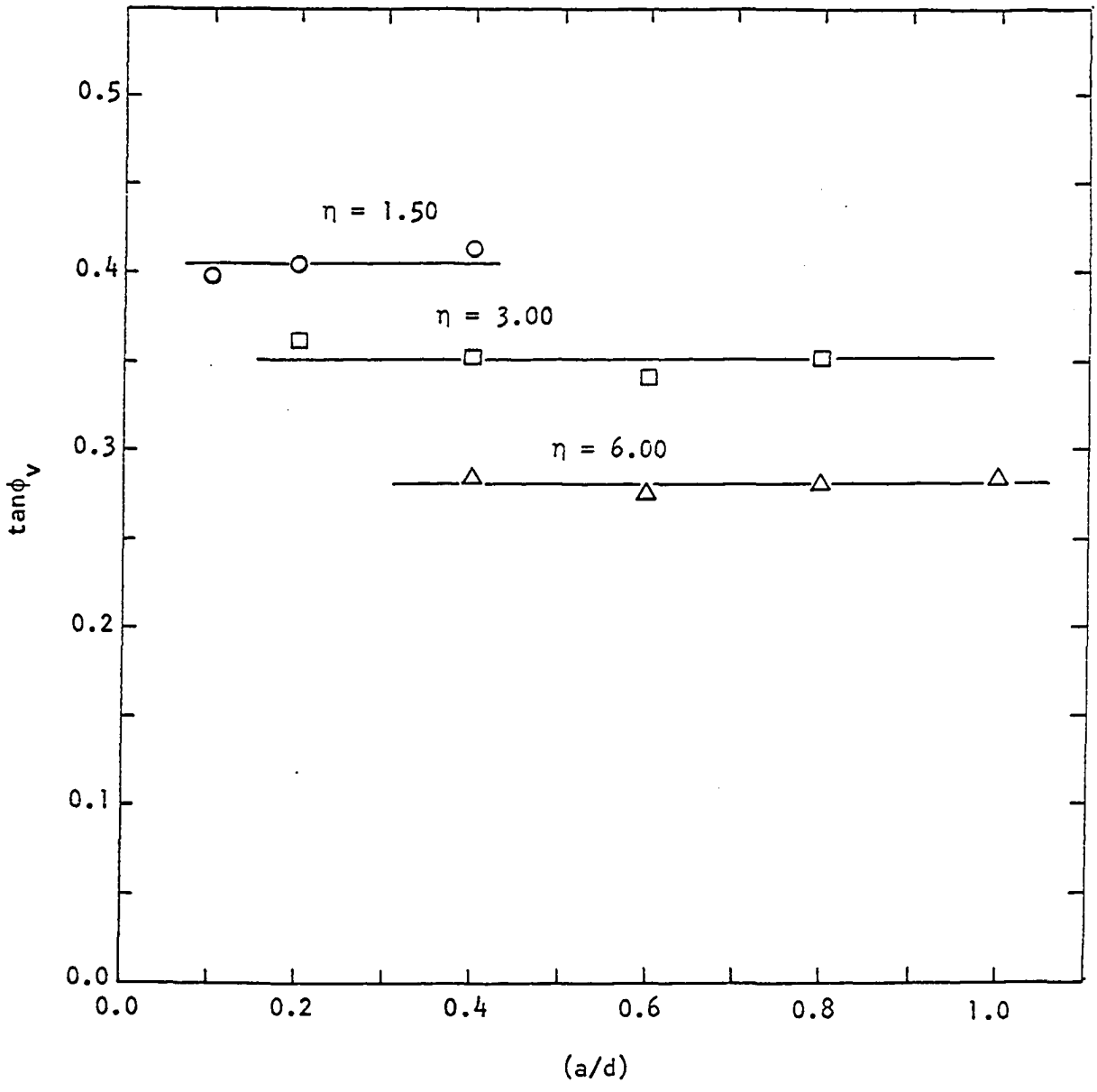

Figure 19. Tanϕ versus the ratio of vibrational amplitude to particle diameter at the EVR condition for 1/16 inch steel balls of 20 psi normal pressure

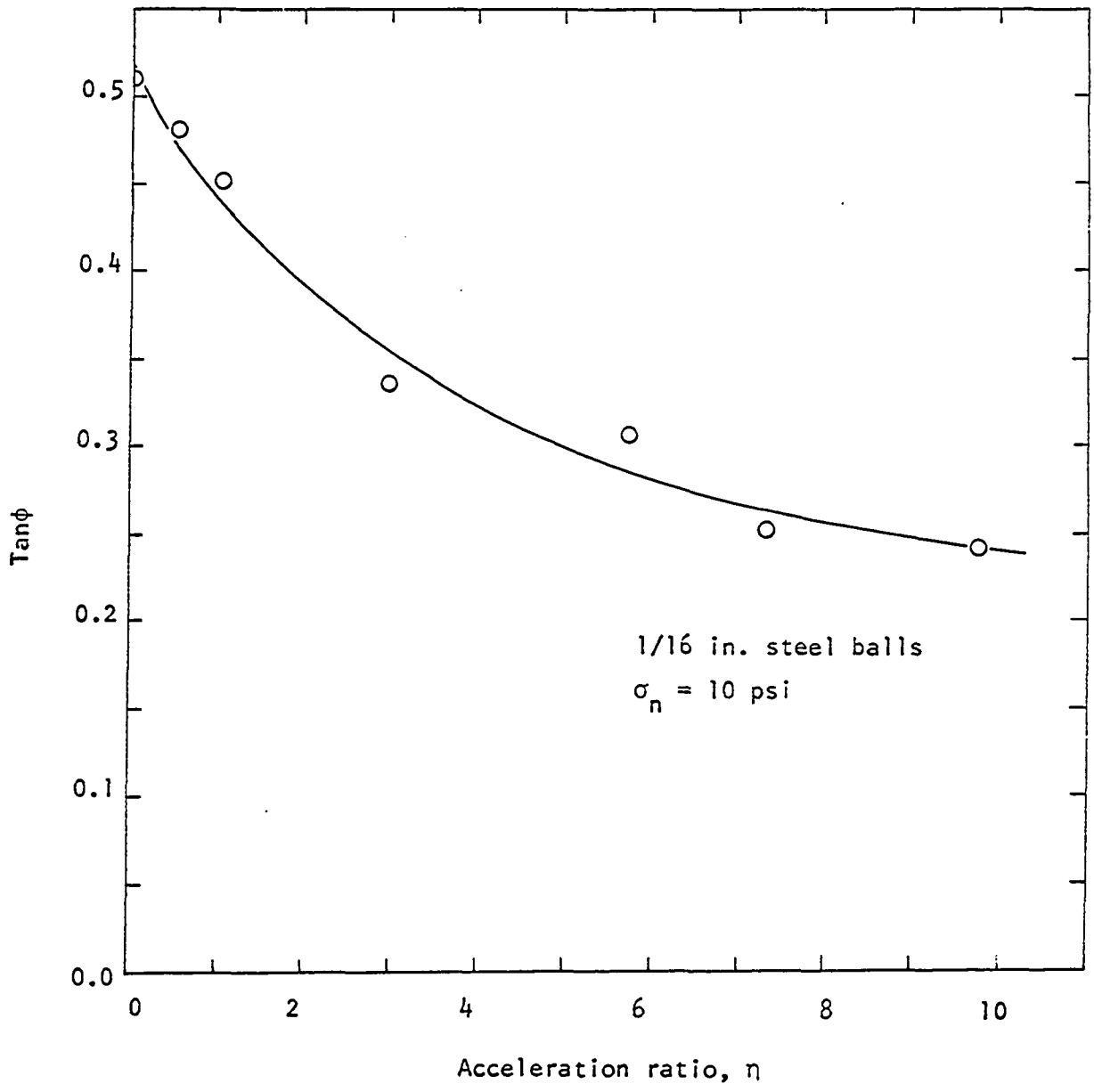

Figure 20. Tanϕ versus acceleration ratio at the EVR condition

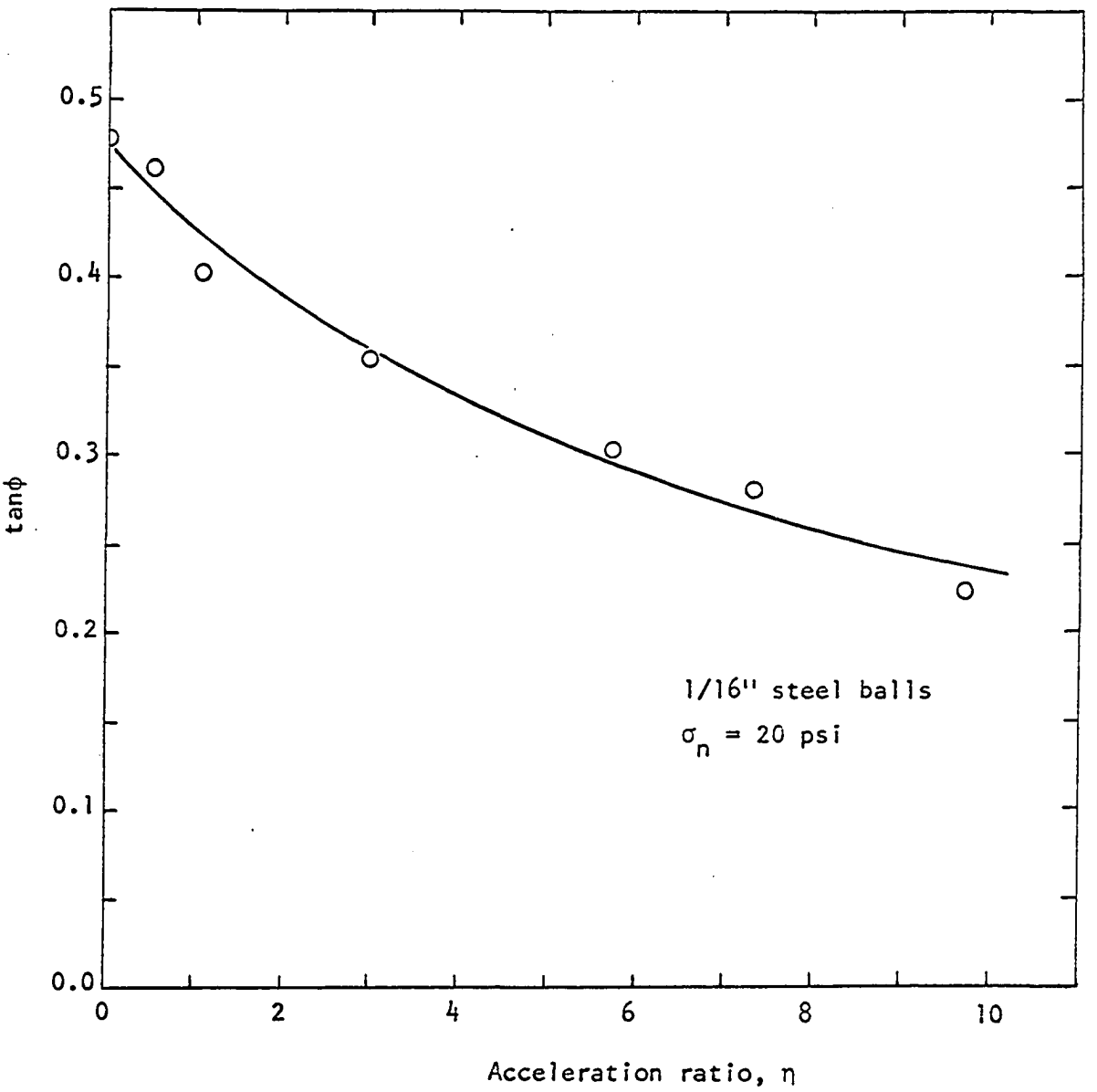

Figure 21. Tanϕ versus acceleration ratio at the EVR condition

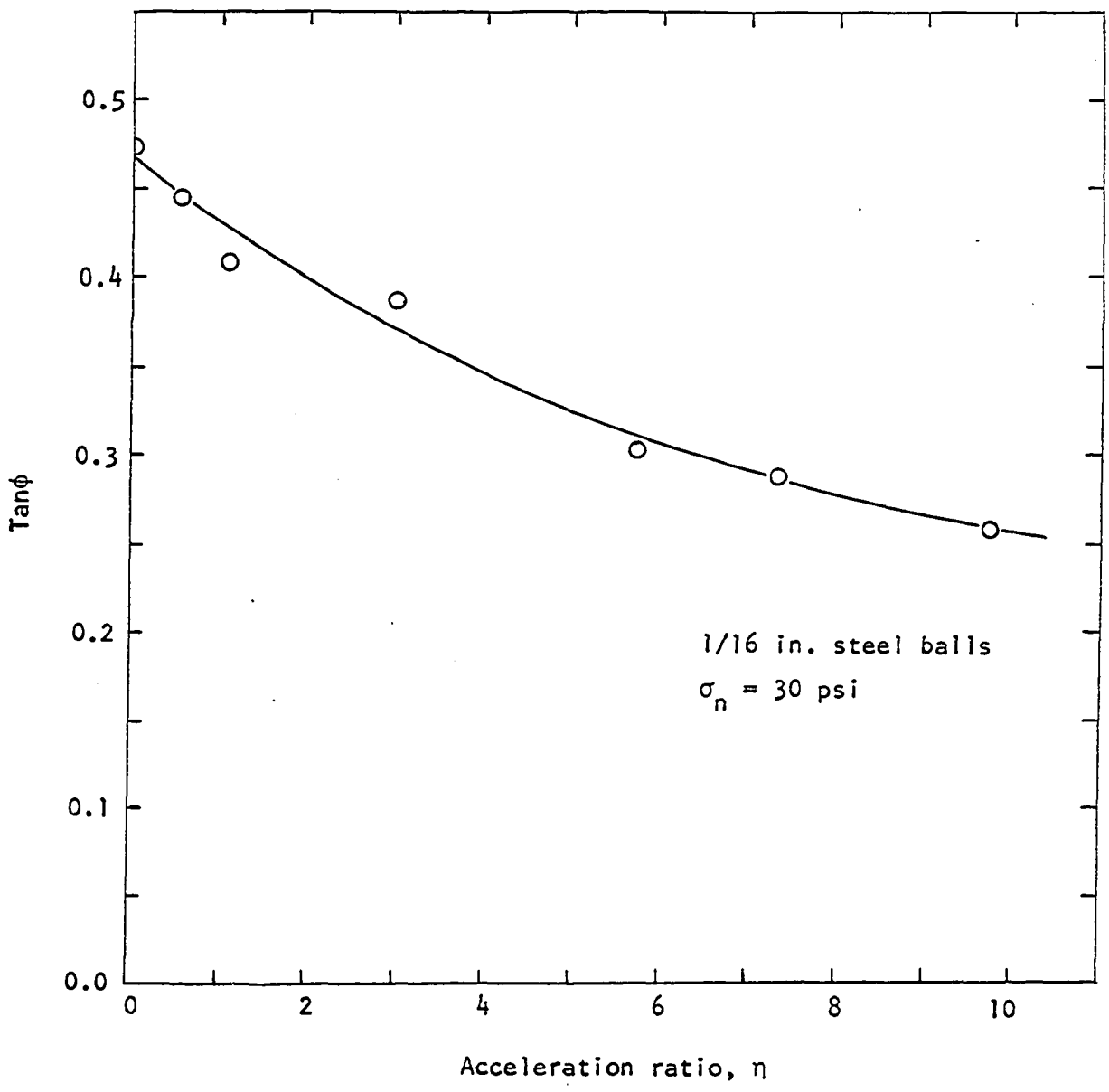

Figure 22. Tanϕ versus acceleration ratio at the EVR condition

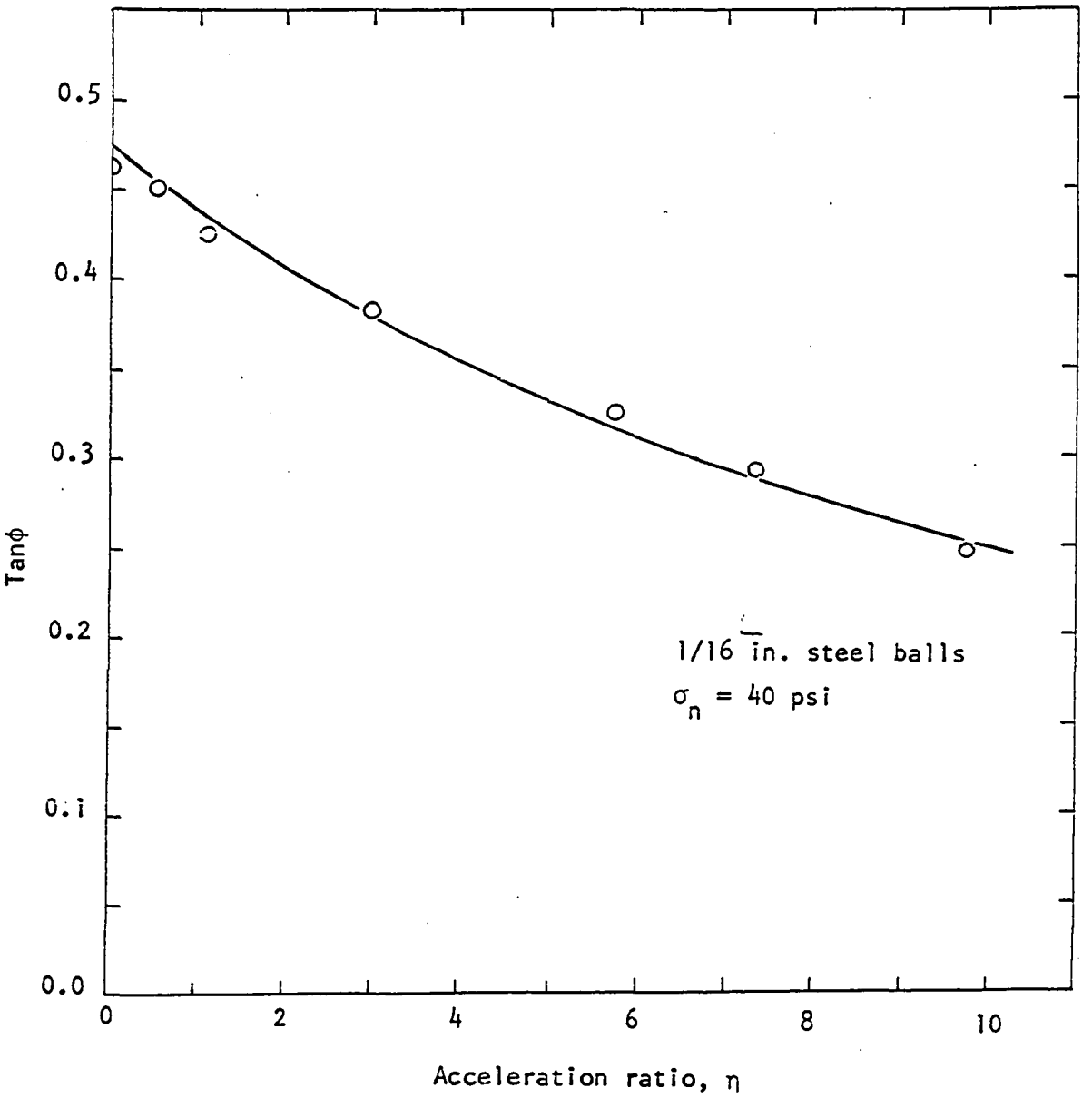

Figure 23. Tanϕ versus acceleration ratio at the EVR condition

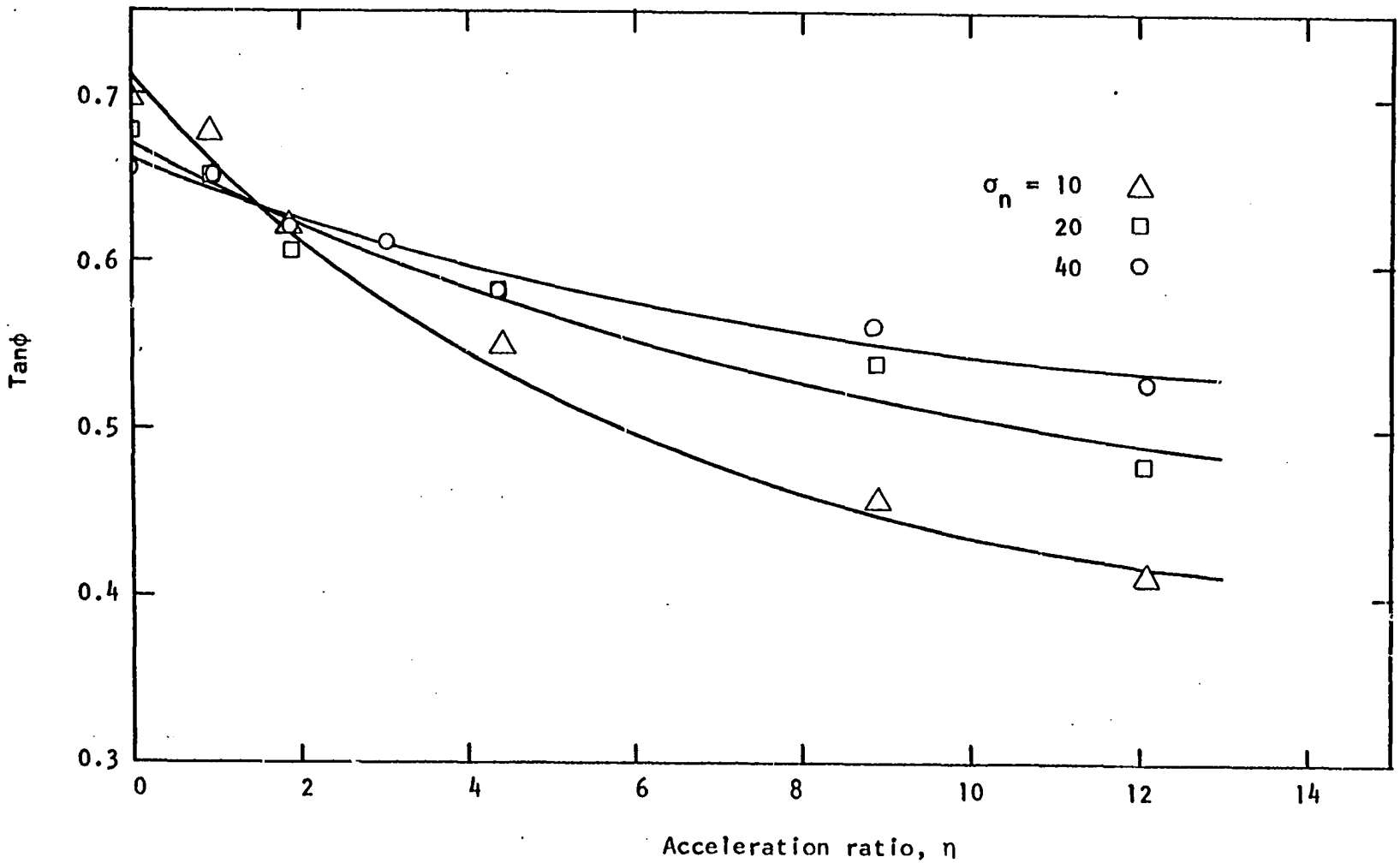

Figure 24. Tanϕ versus acceleration ratio for Ottawa sand at the EVR condition

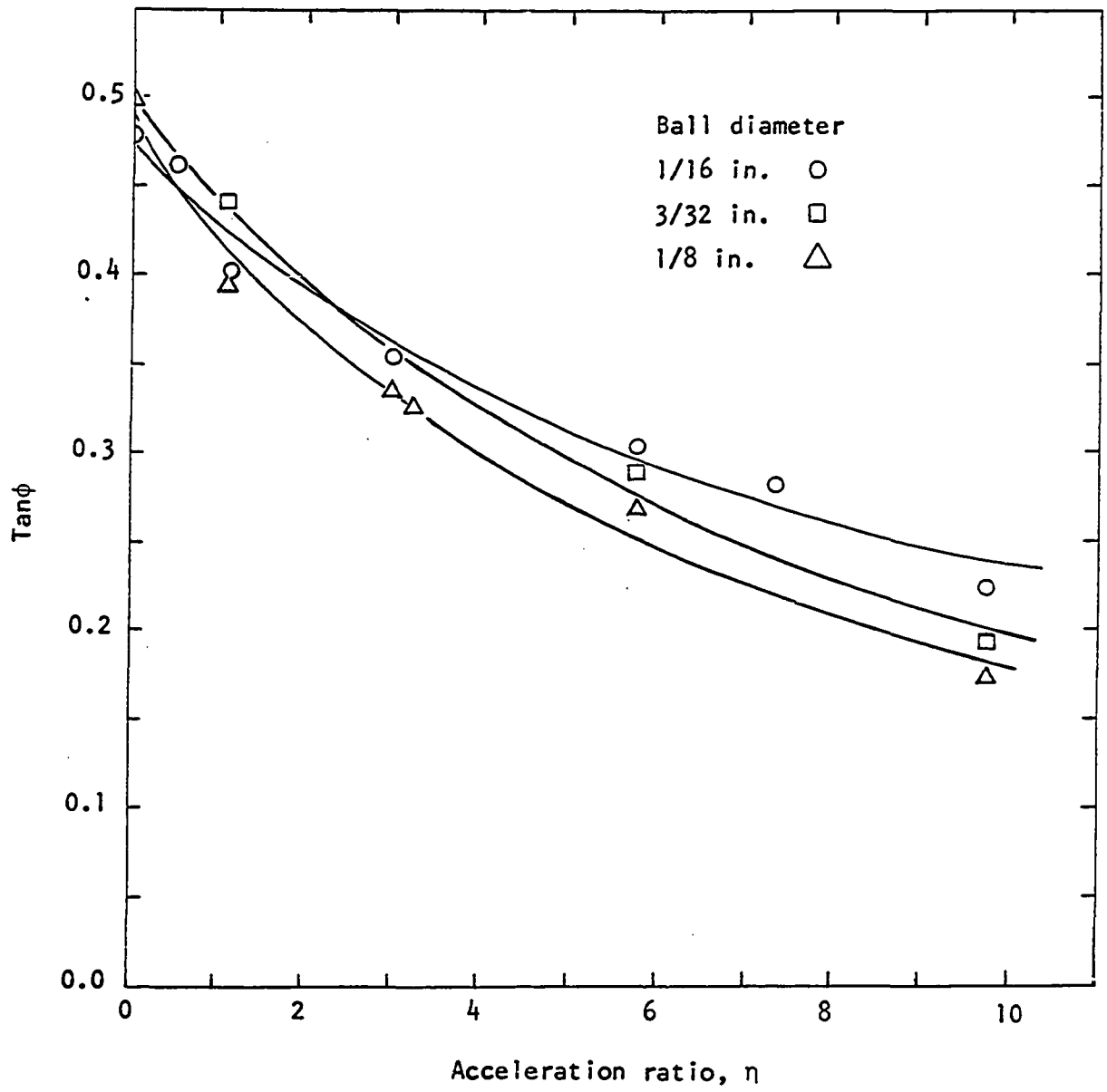

Figure 25. Tanϕ versus acceleration ratio for various sizes of steel balls at 20 psi normal pressure

Table 2. Estimates of $\tan\phi_{st}$, $\tan\phi_{\infty}$ and β, and the correlation coefficient r for shear tests in the EVR condition

Material	σ_n,psi	$\tan\phi_{st}$	$\tan\phi_{\infty}$	β	r
1/16" balls	10.0	0.516	0.220	0.265	0.985
1/16" balls	20.0	.472	.168	.154	.985
1/16" balls	30.0	.467	.186	.139	.993
1/16" balls	40.0	.473	.133	.130	-
3/32" balls	20.0	.493	.019	.091	
1/8" balls	20.0	.480	.105	.164	
sand	10.0	.750	.400	.238	.977
sand	19.1	.708	.461	.153	1.000
sand	20.0	.669	.405	.0935	0.980
sand	40.0	.659	.494	.118	.989

curves it appeared probable that an empirical relationship between β and σ_n could be formulated. This relationship would be of the form:

$$(\beta - 0.12) = (1/\sigma_n)^q \qquad (27)$$

By plotting $\ell n\ (\beta - 0.12)$ against $\ell n\ (1/\sigma_n)$ in figure 28 it was found that for the steel balls the empirical relationship gave a good fit for a value of q of 0.192. Due to lack of data points and scatter of data, no attempt was made to determine the value of q for the sand, but a visual inspection of figure 26 shows that the curve for the balls is a fair estimate for the sand.

Too few sizes of balls and too few shear tests on some of the sizes tested made the data available on the effect of particle size of little value statistically, and they therefore are omitted in this analysis.

In figure 27 the estimates of the parameters $\tan\phi_{st}$ and $\tan\phi_{\infty}$ for sand and 1/16 inch balls are plotted for various normal pressures. The value of $\tan\phi_{\infty}$ is only valid as a parameter in equation 17 and it is not valid as an estimate of the minimum value of the coefficient of internal friction.

It was hypothesized from the theoretical considerations that the EVR and CVR were equivalent. To test this hypothesis the value of the EVR before a shear test and the CVR recorded at the constant volume state of the same test were compared. This was done by computing the value of D for each test, where D is defined by:

$D = e_v - e_c$

e_v = the EVR

e_c = the CVR

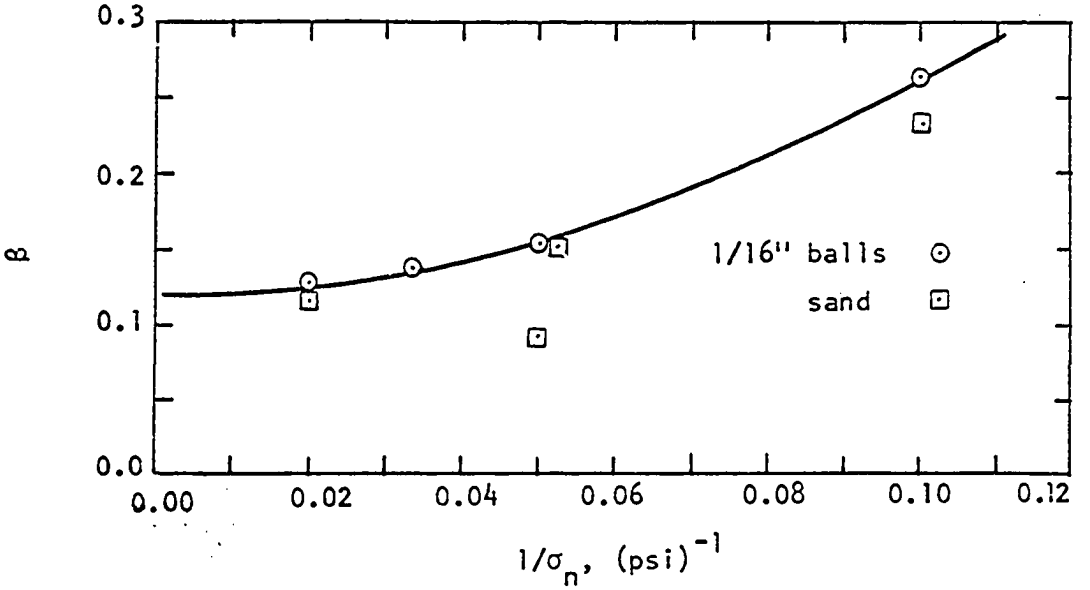

Figure 26. The relationship between β and the reciprocal of the normal pressure

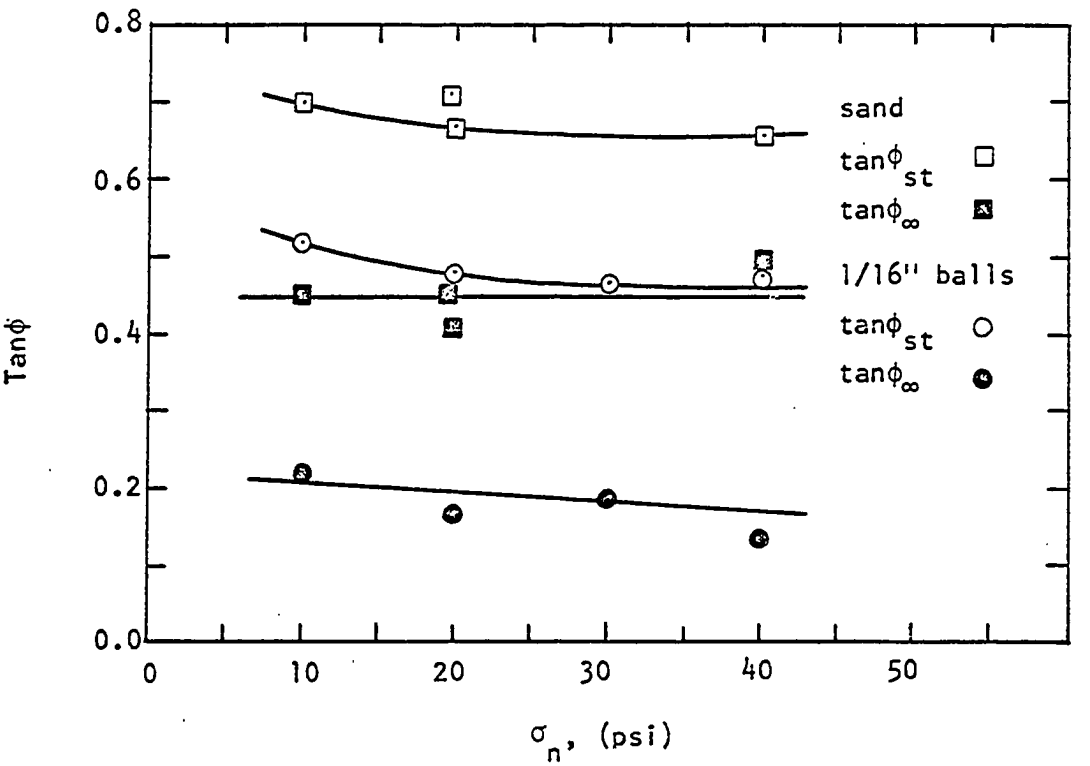

Figure 27. The relationship between the parameters $\tan\phi_{st}$ and $\tan\phi_{\infty}$ and normal pressure for sand and 1/16 inch steel balls

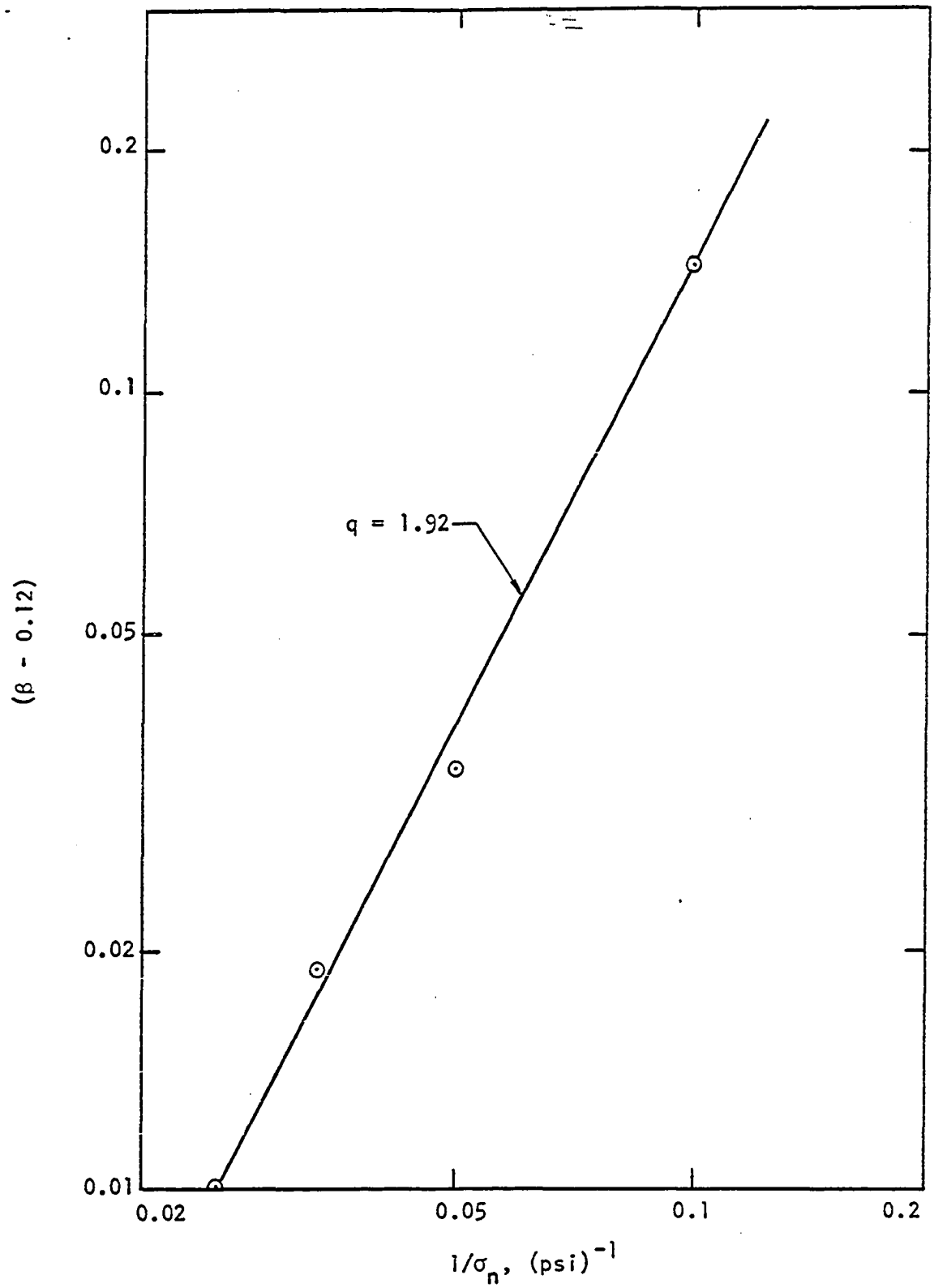

Figure 28. A logarithmic plot of the equation $(\beta - 0.12) = (1/\sigma_n)^q$ for σ_n in psi.

From the hypothesis the mean value of D should be zero. The mean and the standard probable error of D was computed for each series of tests and are tabulated in table 3. The values of e_v and e_c for the tests conducted are tabulated in appendix B.

The results listed in table 3 show that within the limits of experimental accuracy the EVR and the CVR for any particular test are equivalent. Thus the EVR curves shown in figures 12, 13 and 14 are also CVR curves and equation 22 is equally applicable for determining e_c as e_v.

Figure 29 shows the results of shear tests on 1/16 inch steel balls at a variety of initial void ratios, e_o, for a normal pressure of 20 psi and at a frequency of 30 cps. $\text{Tan}\phi_m$ is defined as the maximum coefficient of internal friction. Figure 30 shows similar results for sand with a 19.1 psi normal pressure. In both figures the EVR line is dashed in as a reference. It was impossible to conduct any tests at void ratios greater than the EVR, except for static tests in "unstable equilibrium" and tests in the transient state. The latter were not attempted.

In figure 31 the stress-deformation curves are shown for sand at three different initial void ratios for an acceleration ratio of 3.25. Test 1 was an EVR condition test and is typical of the stress-deformation curves of these tests. This curve shows the equivalence of initial void ratio which was the EVR and the ultimate void ratio which was the CVR. The other two tests show the tendency for a sample at a void ratio less than the EVR to dilate during shear. Since shearing distortion is not uniform throughout the sample in a direct shear test (Lamb, 1951), the void ratio is not necessarily constant throughout the sample after distortion has taken place. This nonhomogeneity of the void ratio was

Table 3. Mean value and standard probable error of D

Material	Normal press. psi	Mean value of D	Standard prob. error of D
1/16" balls	10.0	0.000	0.002
1/16" balls	20.0	- .002	.002
1/16" balls	30.0	- .001	.003
1/16" balls	40.0	.000	.003
1/16" balls	all tests	- .001	.003
sand	10.0	.003	.004
sand	19.1	.000	.003
sand	20.0	.002	.001
sand	40.0	.001	.002
sand	all tests	.001	.003

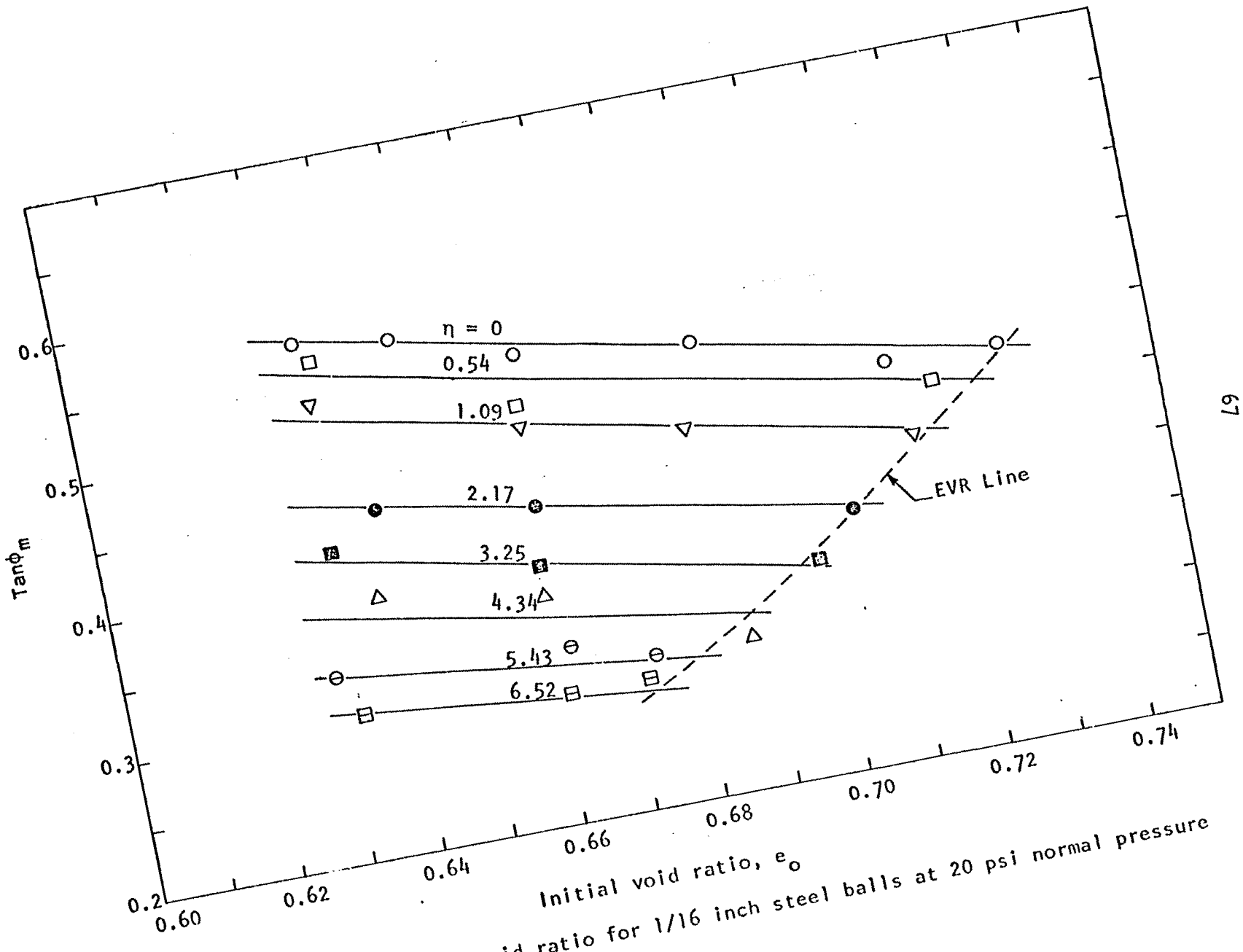

Figure 29. $\text{Tan}\phi_m$ versus void ratio for 1/16 inch steel balls at 20 psi normal pressure and a frequency of 30 cps

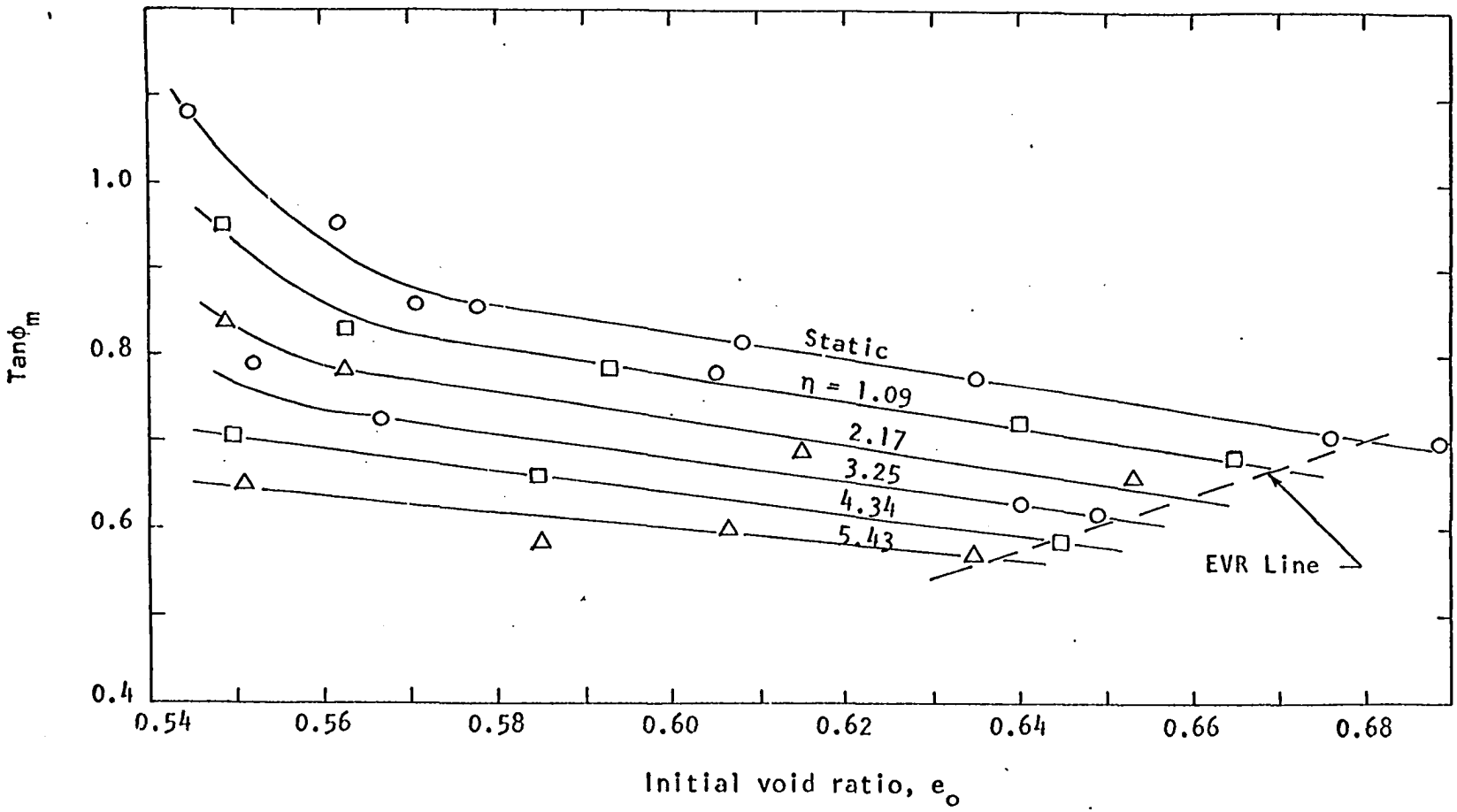

Figure 30. Tanϕm versus initial void ratio for Ottawa sand at 19.1 psi normal pressure and a frequency of 30 cps

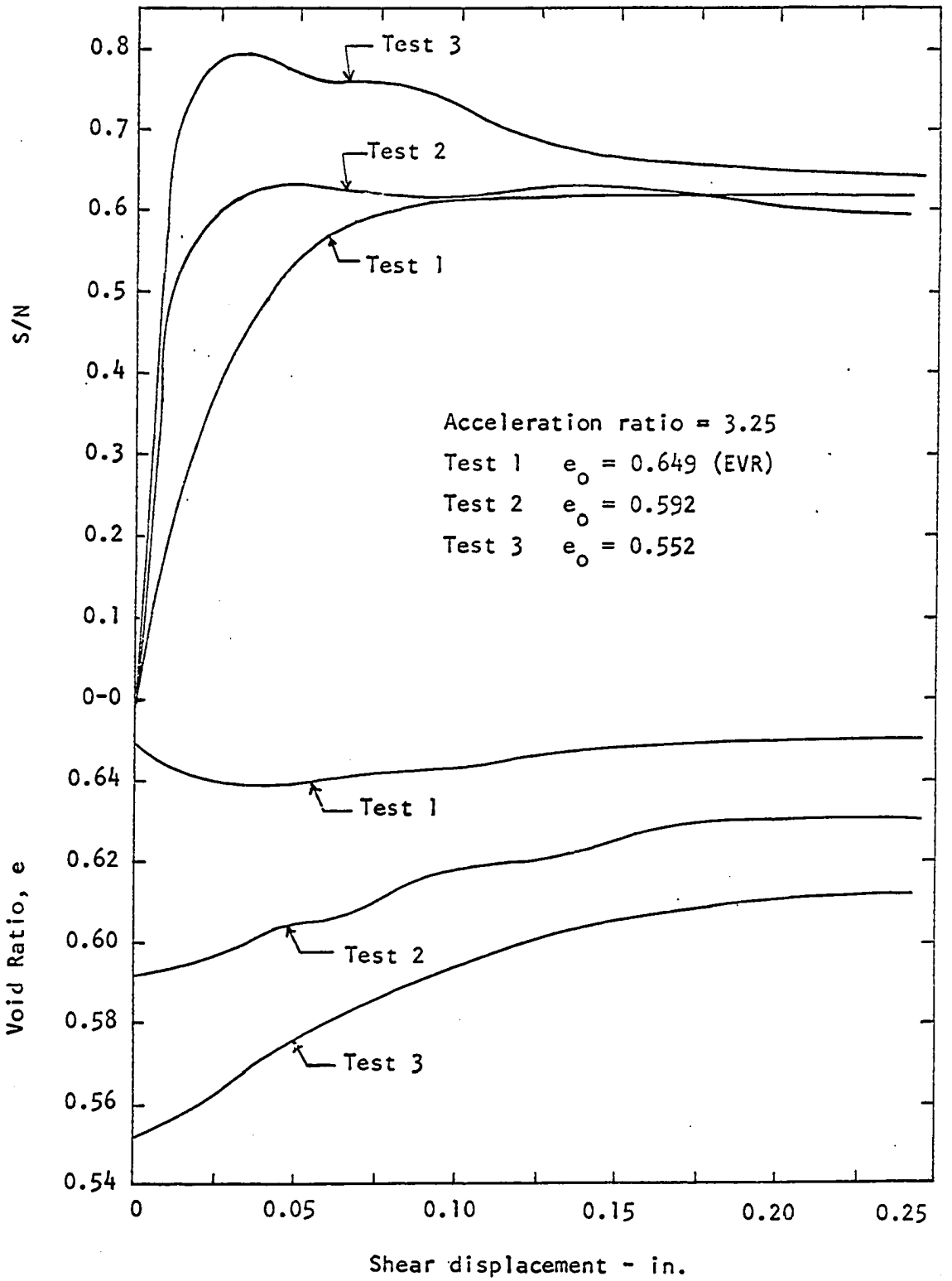

Figure 31. The effect of initial void ratio on the shear strength and dilatation of sand subjected to vibration

probably responsible for the observed result, that when all other conditions remained constant, the lower the initial void ratio, the lower the void ratio at the constant volume state as shown in figure 31. However, the variation of the void ratio throughout a sample would be minimal for tests where the initial and final void ratio were near the same value. This corresponds to the EVR-CVR condition and thus the error in the computed CVR would be minimal, and this effect was neglected.

In figure 32 the results of tests on sand with initial void ratios less than the EVR are shown. In figure 33 the results of similar shear tests on 1/16 inch steel balls are shown. The curves are typical of the results for shear tests at a void ratio less than the EVR. The data from these tests and other tests not plotted were analyzed with the aid of the electronic computer using the "Modified Gauss-Newton" method for nonlinear regression as previously described. In this case the regression model fitted was equation 18 and the parameters estimated were $\tan\phi_{st}$, A and β_2. These estimates are tabulated in table 4.

The results for several of the shear tests at void ratios less than the EVR were separated into components due to frictional resistance and interlocking by equation 5. These results are tabulated in the appendix. In figures 32 and 33 typical results of the frictional and interlocking components are shown. These results show that both interlocking and frictional resistance are reduced by vibration.

The effect of vibration on the ultimate coefficient of internal friction, $\tan\phi_u$, is shown in figure 34. This shows that $\tan\phi_u$ was also reduced by vibration. It was also observed that the coefficient of internal friction in the ultimate state approaches the corresponding EVR

Table 4. Estimates of $\tan\phi_{st}$, A and β_2, and the correlation coefficient r for non-EVR shear tests

Material	σ_n, psi	e_o	$\tan\phi_{st}$	A	β_2	r
1/16" balls	10.0	0.66	0.59	0.21	0.23	0.99
1/16" balls	20.0	.66	.55	.23	.27	.83
1/16" balls	40.0	.66	.50	.26	.17	.99
1/16" balls	20.0	.63	.57	.02	.24	.99
1/16" balls	40.0	.63	.55	.36	.31	.96
sand	10.0	.61	.88	.26	.16	1.00
sand	20.0	.61	.86	.49	.25	1.00
sand	40.0	.61	.86	.55	.22	0.98
sand	10.0	.58	.96	.38	.20	.99
sand	20.0	.58	.95	.51	.33	.97
sand	40.0	.58	.95	.52	.18	.99

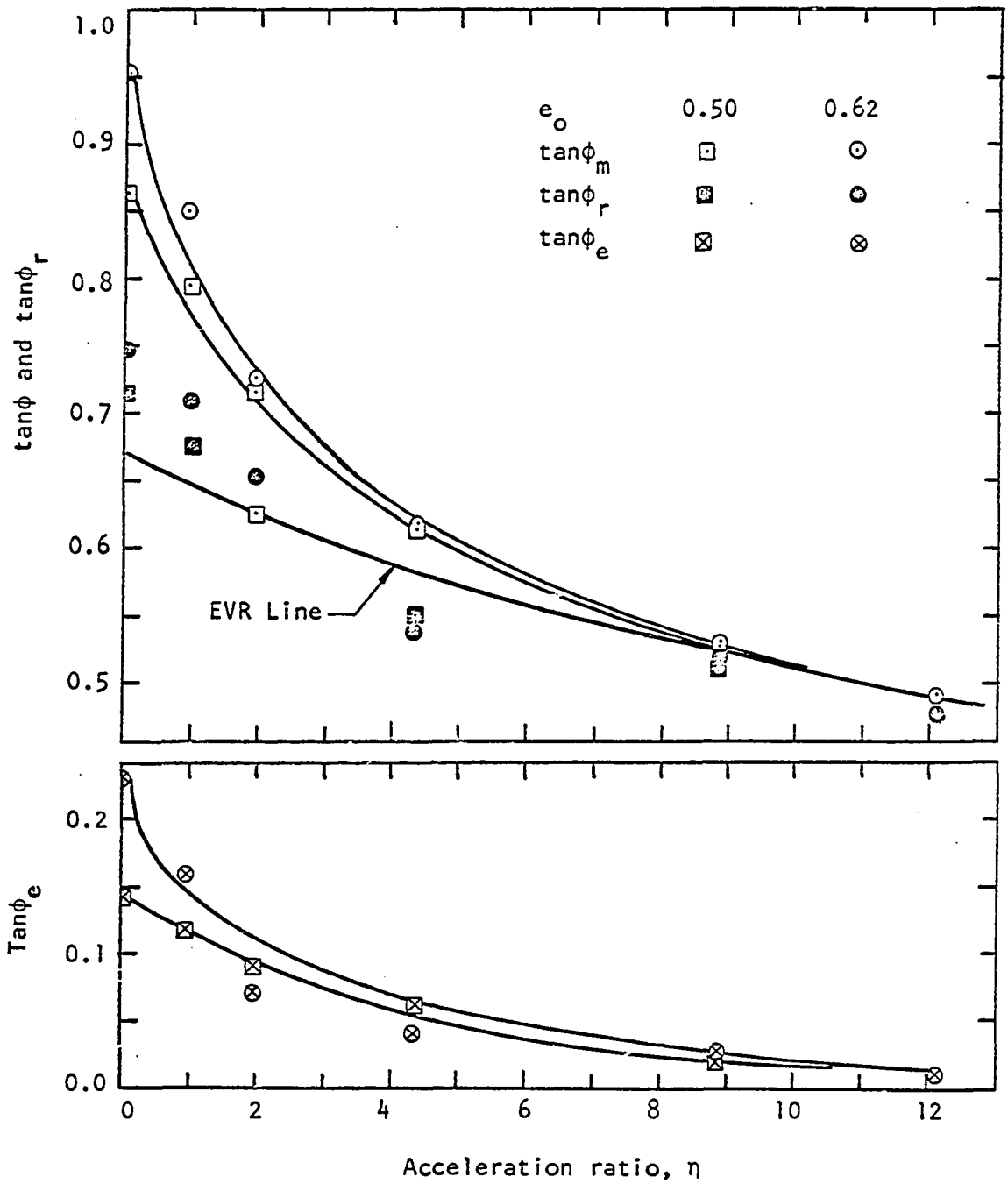

Figure 32. The effect of vibration on the maximum coefficient of internal friction ($\tan\phi_m$), frictional resistance ($\tan\phi_r$), and interlocking ($\tan\phi_e$) for Ottawa sand

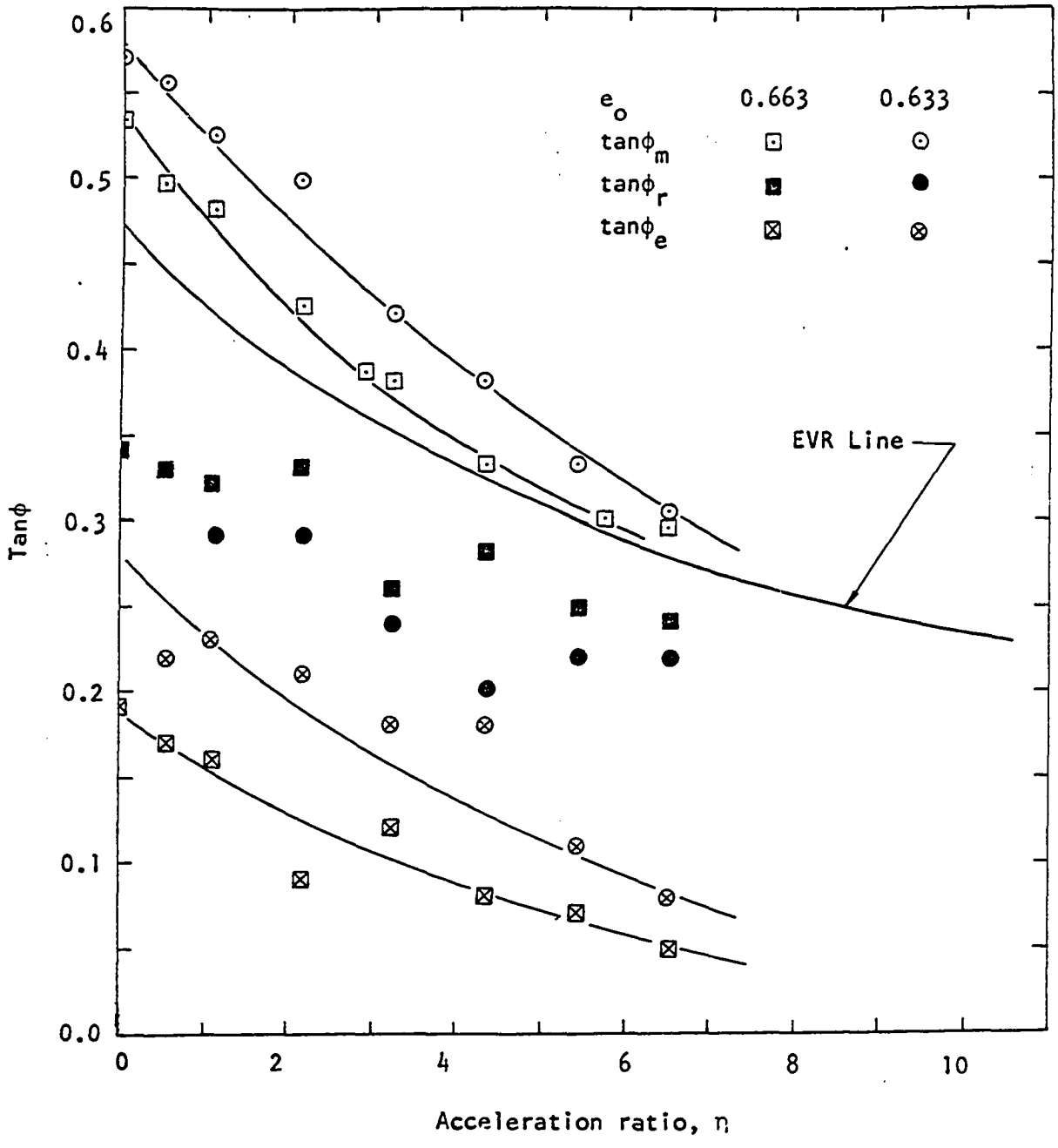

Figure 33. The effect of vibration on the maximum coefficient of internal friction ($\tan\phi_m$), frictional resistance ($\tan\phi_r$) and interlocking ($\tan\phi_e$) for 1/16 inch steel balls

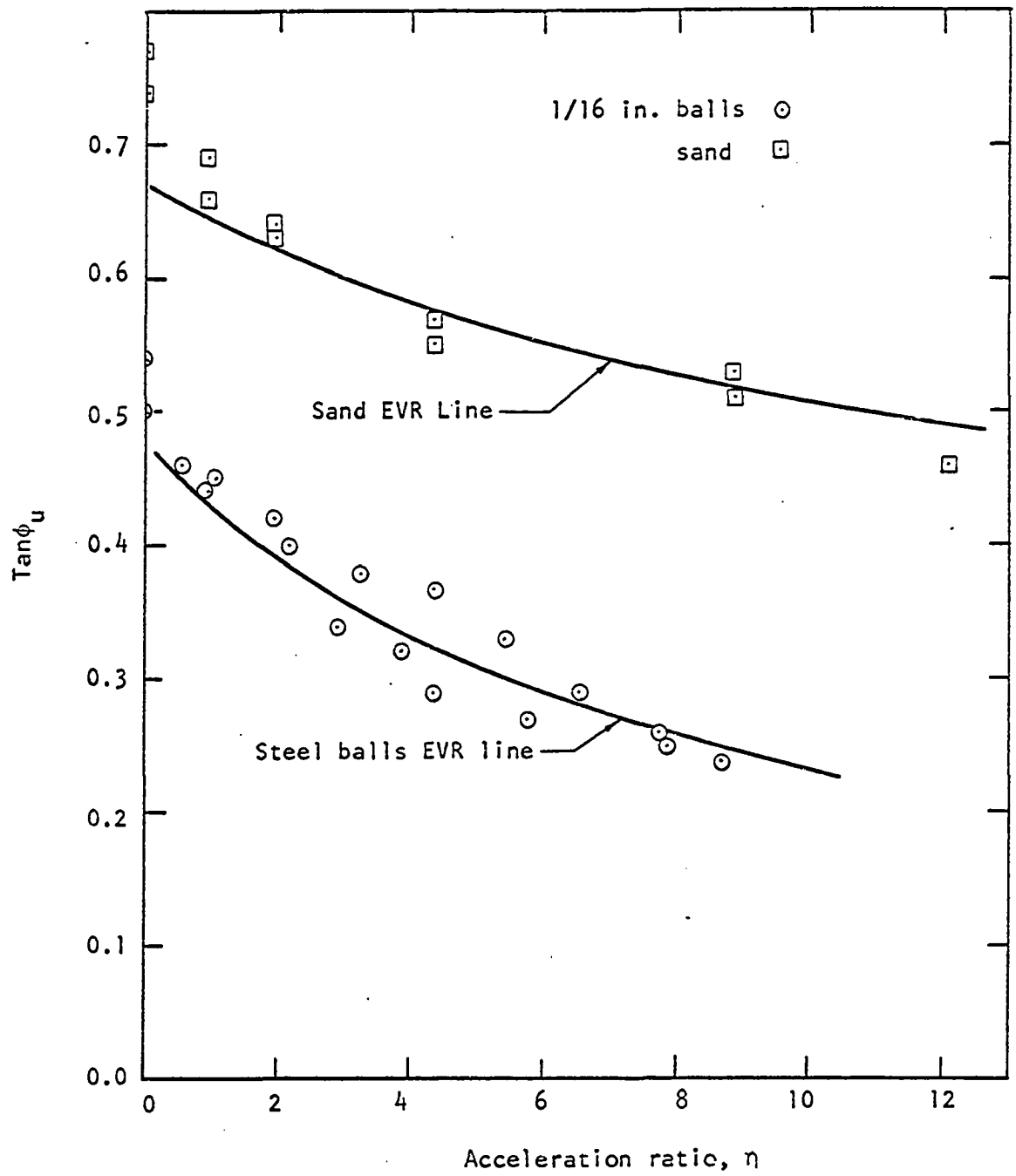

Figure 34. The effect of vibration on the ultimate coefficient of internal friction of sand and 1/16 inch steel balls at 20 psi normal pressure

coefficient. It is probable that not all of the tests were in the ultimate state when the test was discontinued due to deformation limitations of the apparatus, and therefore some of the values plotted may be greater than the actual $\tan\phi_u$.

VI. SUMMARY AND DISCUSSION

The experimental results were in agreement with the results which were predicted from the theoretical mechanisms proposed in the chapter on theoretical considerations. The results of this investigation in general confirmed the results reported by Barkan (1962) on the same properties with the exception of one observation which is discussed later in this chapter.

The EVR, which was defined as the ultimate void ratio of a granular system densified by a particular vibration, decreased as vibrational acceleration increased. The relationship between the EVR and acceleration of vibration was theoretically determined (equation 22) and was found to be valid for all of the tests conducted. The coefficient of vibratory compaction α, which is one of the parameters of equation 22, was found to decrease with increased normal pressure. An empirical relationship between α and the normal pressure was formulated (equation 26). The experimental values of α fit this equation very well for the 1/16 inch steel balls; however, much less confidence could be placed in the fit for the sand due to scatter of the data.

The coefficient of internal friction was reduced by vibration, as predicted. For shear tests on samples in the EVR condition the theoretically determined equation 17 was found to be valid for the tests conducted. It was found that the coefficient of shear strength reduction β decreased with increased normal pressure. An empirical relationship between β and the normal pressure was formulated (equation 27) which fit the data for the 1/16 inch steel balls very well. Due to scatter and lack of data, fitting

---

[1] A list of symbols used in this thesis is given in appendix A.

the data for the sand to this relationship was not attempted.

For shear tests on samples with initial void ratios less than the EVR it was found that both the maximum and ultimate coefficient of internal friction were reduced by vibration, and that both the frictional and interlocking components were reduced. Equation 18, which was intuitively assumed from the form of equation 17, was found to be valid in predicting the maximum coefficient of internal friction. The coefficient of internal friction for tests in the ultimate state was found to approach the coefficient for the EVR condition.

It was found that the initial void ratio for a shear test on a sample in the EVR condition and the void ratio at the ultimate constant volume state of the same test were equivalent. Since the latter, void ratio, is defined as the critical void ratio (CVR), the EVR and the CVR were found to be equivalent.

In the range of accelerations and normal pressures investigated, the effect of vibration tended to be counteracted by an increase of normal pressure. This effect of normal pressure can be explained by the mechanisms proposed in the chapter on theoretical considerations. The greater the normal pressure, the more tightly the particles are held in place by the frictional and interlocking forces. If a system of particles acted upon by a particular vibration is subjected to a sufficiently low normal pressure, there would be enough relative motion between particles to reduce the energy barriers to a minimum, thus allowing particles to be moved with much less applied inertial or shear force. On the other hand, if the same system were subjected to a very high normal pressure the particle contact pressures would be so great that very little relative

motion between particles could occur, and there should be very little reduction of the energy barriers.

One implication of the above finding could be in opposition to the following statement made by Barkan (1962). "The tests also showed that as normal pressure grows, the changes of porosity produced by shear decrease." It follows from the argument of the preceding paragraph that the amount of reduction of the CVR would decrease with increased normal pressure. Thus, even though statically the CVR decreases with increased normal pressure, the reverse could be true under vibratory conditions. This was experimentally found to be the case. In the range of normal pressures tested, for acceleration ratios greater than about 0.5 for the 1/16 inch steel balls and 1.0 for sand, the CVR increased with increased normal pressure. It was concluded previously that a sample initially at a void ratio less than the CVR dilates during shear distortion, ultimately approaching the CVR; therefore, in the cases where the CVR increases with normal pressure, dilatation would increase with normal pressure. This is shown by a set of typical void ratio-deformation curves (figure 35) obtained in this investigation for a constant initial void ratio and vibrational acceleration but varying normal pressure.

The significance of the results of this investigation can be illustrated with some hypothetical examples.

First consider the case of a static load, such as a building, supported on a mass of cohesionless material which has vibrational properties similar to the materials used in this investigation. Let us further stipulate that the initial void ratio throughout the mass is less than the static CVR and that the load supported by the mass is stable. If

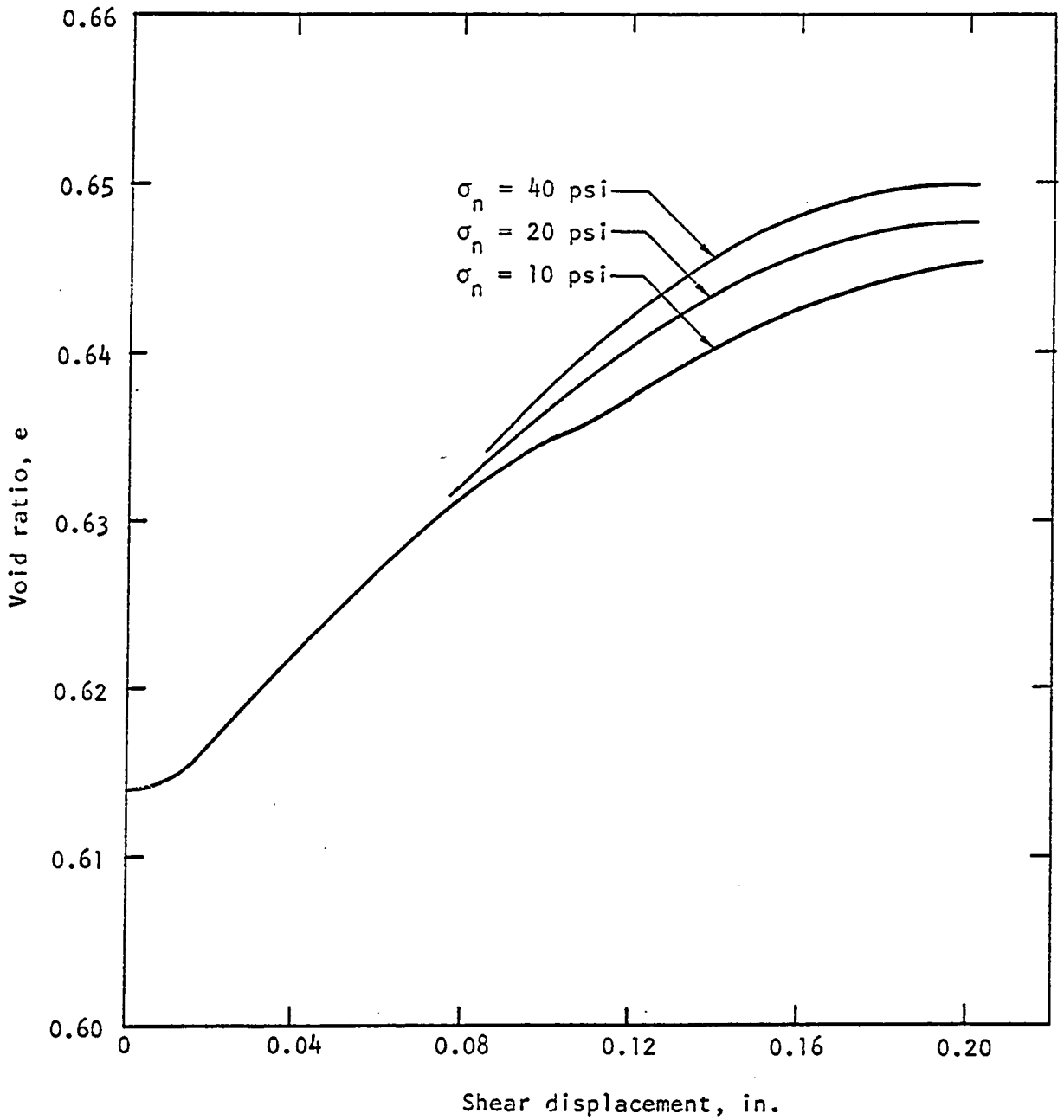

Figure 35. Dilatation of Ottawa sand at an acceleration ratio of 2.17

the mass and load are then subjected to vibration, for example by an earthquake, several effects of the vibration occur. First, the shear strength of the supporting soil would be reduced, which could lead to a shear failure. Second, the amount of dilatation which would occur during a shear failure would be reduced. If the vibrational acceleration on the system reaches the intensity necessary to produce the EVR condition, no dilatation at all would occur. Third, if the acceleration of vibration were to exceed that of the EVR condition, densification of the soil accompanied by settlement would occur. If in the latter case the problem were compounded by a saturated soil condition, densification might occur faster than pore water pressures could dissipate, leading to a state of liquifaction.

In the example cited above all of the devastating effects could occur even though the initial void ratio was less than the static CVR and the building was statically stable. In summary, vibration causes a reduction of shear strength, decreased dilatency, and for accelerations greater than the EVR condition acceleration, densification and settlement. This is evidenced in the field by the frequent occurence of settlement and land slides in granular materials when subjected to vibration such as from an earthquake, piie driving operation, industrial machinery, etc.

Next consider the case of a granular material, of the type investigated, initially in its loosest possible condition. If a source of vibration, such as a vibratory compactor, is placed somewhere on or in the material, waves will be propagated from the source and dissipate with distance. Thus the acceleration at any point in the soil will depend on its position relative to the vibrator. The normal pressure at the point

would also be a function of its position. With this information, the results of this investigation could be applied to determine the ultimate density at any point in the soil. If the material were initially at some void ratio less than it's loosest possible condition, the sphere of densifying influence would be that sphere in which the vibrational acceleration was greater than that necessary to produce the EVR condition. The boundary surface of this region would thus be a function of the initial void ratio, normal pressure and acceleration acting at any particular point on the boundary.

VII. CONCLUSIONS

The following conclusions are based on experimental test results on uniformly graded steel balls and rounded silica sand:

1. The void ratio ultimately attained by a loose granular material subjected to steady state vibration, which was termed the vibrational equilibrium void ratio (EVR), is also the critical void ratio (CVR) for the material if sheared while subjected to this same vibration.

2. The EVR, and thus the CVR, decreases with increased vibrational acceleration. For the range of accelerations investigated this relationship is expressed by equation 22.

3. The coefficient of internal friction for a material in the EVR condition was reduced by vibration and is related to the acceleration by equation 17.

4. Both the maximum and ultimate coefficients of internal friction were reduced by vibration. Also, both the frictional and the interlocking components of the shear strength were reduced by vibration.

5. The effects of vibration on the properties and phenomena investigated were a function of only one vibrational parameter--the acceleration.

6. An increase of normal pressure tended to counteract the effects of the vibration in all instances investigated.

VIII. SUGGESTIONS FOR FURTHER RESEARCH

The following areas for further research are suggested:

1. A study of the factors effecting the rate of vibratory densification.

2. An investigation of the effect of moisture content on the results of this investigation.

3. A study of the influence of the material properties on the effect of vibration.

4. A study of the applicability of the results of this investigation to the case of vibrations caused by oscillating normal stresses.

IX. LITERATURE CITED

American Society for Testing and Materials. Committee D-18 on Soils and Rocks for Engineering Purposes. 1964. Procedures for testing soils. Philadelphia, Pa., author.

Amontons, [G] 1699. De la resistance causeé dans le machines. Acadamie Royale des Sciences, Paris, France, Historie avec le Mémoires de Mathématique et de Physique 1699:209-277.

Atkinson, J. D. 1966. Tarsier reference manual. Iowa State University of Science and Technology Statistical Laboratory Numberical Analysis Programming Series, No. 8.

Barkan, D. D. 1962. Dynamics of bases and foundations. New York, N.Y., McGraw-Hill Book Co., Inc.

Bowden, F. P. and D. Tabor. 1950. The friction and lubrication of solids. London, England, Oxford University Press.

Converse, F. J. 1962. Foundations subjected to dynamic forces. In Leonards, G. A. ed. Foundation engineering. pp. 769-824. New York, N.Y., McGraw-Hill Book Co., Inc.

Coulomb, C. A. 1781. Theorie des machines simples, en ayant égard an frottement de lewrs parties, et a la roideur des cordages. Acadamie Royale des Sciences, Paris, France, Mémoires de Mathématique et de Physique 10, No. 2:161-332. 1785.

D'Appolonia, E. 1953. Loose sands: their compaction by vibroflotation. American Society for Testing and Materials Special Technical Publication 156:138-154.

Eyring, H. and R. E. Powell. 1944. Rheological properties of simple and colloidal systems. Alexander's Colloid Chemistry 5:236-252.

Goodman, L. J., A. R. Aidum, and C. S. Grove, Jr. 1965. Soil surface compaction with foam-type explosives. American Society of Civil Engineers Proceedings 91, No. SM1:143-165.

Hartley, H. O. 1961. The modified Gauss-Newton method for the fitting of non-linear regression functions by least squares. Technometrics 3:269-280.

Idriss, I. M. and H. B. Seed. 1967. Response of earth banks during earthquakes. American Society of Civil Engineers Proceedings 93, No. SM3:61-82.

Johnson, A. W. and J. R. Sallberg. 1960. Factors that influence field compaction of soils. Highway Research Board Bulletin 272.

Krey, H. 1932. Erddruck, Erdwiderstand und Tragfähigkeit des Baugrundes Berlin, Deutschland, Wilhelm Ernst ahd Sohn.

Lamb, T. W. 1951. Soil Testing for engineers. New York, N.Y., John Wiley and Sons, Inc.

Leonards, G. A. 1962. Engineering properties of soils. In Leonards, G. A. ed. Foundation engineering. pp. 66-240. New York, N.Y., McGraw-Hill Book Co., Inc.

Linger, D. A. 1963. Effect of vibration on soil properties. Highway Research Record 22:10-22.

MacCurdy, E. 1938. The notebooks of Leonardo da Vinci. Vol. 1. New York, N.Y., Reynal and Hitchcock.

Major, A. 1962. Vibration analysis and design of foundations for machines and turbines. London, England, Collet's Holdings, Ltd.

Means, R. E. and J. V. Parcher. 1963. Physical properties of soils. Columbus, Ohio, Charles E. Merrill Books, Inc.

Mencl, V. and J. Kazda. 1957. Strength of sand during vibration. International Conference on Soil Mechanics and Foundation Engineering, Fourth, Proceedings 1:382-383.

Mogami, T. and K. Kubo. 1953. The behavior of sand during vibration. International Conference on Soil Mechanics and Foundation Engineering, Third, Proceedings 1:152-155.

Moore, W. J. 1963. Physical chemistry. 3rd ed. Englewood Cliffs, N.J., Prentice-Hall, Inc.

Murphy, G. 1950. Similitude in engineering. New York, N.Y., The Ronald Press Co.

Reynolds, O. 1885. On the dilatency of media composed of rigid particles in contact. Philosophical Magazine Series 5, 20:469-481.

Roscoe, K. H., A. N. Schofield and C. P. Wroth. 1958. On the yielding of soils. Geotechnique 8, No. 1:22-57.

Scott, R. F. 1963. Principles of soil mechanics. Reading, Mass., Addison-Wesley Publishing Co., Inc.

Seed, H. B. and I. M. Idriss. 1967. Analysis of soil liquifaction: Nigata earthquake. American Society of Civil Engineers Proceedings 93, No. SM3:93-108.

Selig, E. T. 1963. Effect of vibration on density of sand. Panamerican Conference on Soil Mechanics and Foundation Engineering Second, Proceedings 1:129-144.

Spanovich, M. 1964. Vibratory maximum density [by] H. C. Pettibone and J. Hardin: [discussion]. American Society for Testing and Materials Special Technical Publication 377:20-30.

Tabor, D. 1959. Junction growth in metalic friction. Royal Society Proceedings Series A, 251:378-393.

Taylor, D. W. 1948. Fundamentals of Soil Mechanics. New York, N.Y., JOhn Wiley and Sons, Inc.

Terzaghi, K. 1925. Erdbaumechanik auf bodenphysikalischer Grundlage. Wien, Österreisch, F. Deuticke.

Tinoco, F. H. 1967. Shear strength of granular materials. Unpublished Ph.D. thesis. Ames, Iowa, Library, Iowa State University of Science and Technology.

Viering, G. 1961. The vibrational behavior of soil in relation to its properties. International Conference on Soil Mechanics and Foundation Engineering, Fifth, Proceedings 1:547-552.

Winterkorn, H. F. 1953. Macromeritic liquids. American Society for Testing and Materials Special Technical Publication 156:77-89.

Yong, R. N. and B. P. Warkentin. 1966. Introduction to soil behavior. New York, N.Y., The Macmillan Co.

X. ACKNOWLEDGEMENTS

A National Science Foundation Traineeship was the source of funds used to purchase the necessary equipment for this project. The Traineeship also provided a stipend for my personal expenses. For this essential financial aid I am sincerely grateful.

The facilities and equipment of the Engineering Research Institute were freely made available to me. This provided another essential contribution to this research project which was greatly appreciated.

Of great assistance was the advice, interest and suggestions of Dr. Richard L. Handy who was the authors major professor. The interest and suggestions of other associates at the university were also very beneficial to me.

A special note of appreciation is due to a patient and thoughtful wife for her encouragement and condolences during the course of this research project.

And finally, I am grateful to Him who gave me strength, intellect and inspiration to complete this work.

XI. APPENDIX A. NOTATION

The following symbols are used in this thesis.

a = the amplitude of vibration.

A = a dimensionless parameter in equation 18.

A' = the area of real contact between two surfaces.

d = the particle diameter.

D = the difference between e_v and e_c for a particular test.

$\underline{e}$ = the base of natural logarithms.

e = the void ratio.

e_c = the critical void ratio (CVR)

e_{max} = the maximum stable void ratio under static conditions.

e_{min} = the limiting minimum void ratio.

e_o = the initial void ratio.

e_v = the vibrational equilibrium void ratio (EVR).

e_∞ = a parameter obtained from an extrapolation of the $e_v - \eta$ curve to a value of η approaching infinity.

E = the modulus of elasticity of the particles.

f = the coefficient of friction.

f' = the frequency of vibration, cycles per second.

g = the acceleration of gravity.

Δh = the change in sample height caused by an incremental shear distortion $\Delta\delta$.

H = the sample height.

H_s = the equivalent height of the solids.

M = a general term representing all the material properties of a system of particles.

N = the normal load

p = the normal pressure per unit of real contact area and also the yield pressure of the material.

p = an exponential constant in equation 26.

q = an exponential constant in equation 27.

r = the correlation coefficient.

s' = the shear strength per unit area of the molecular bonds.

S = the shearing resistance.

S_m = the maximum shearing resistance.

α = the coefficient of vibratory compaction.

β = the coefficient of shear strength reduction.

β_2 = the coefficient of shear strength reduction for a non-EVR condition test.

δ = the effect of vibration $(\tan\phi_{st} - \tan\phi)/\tan\phi_{st}$.

$\Delta\delta$ = an increment of shear distortion.

η = the vibrational acceleration ratio.

π_M = pi-terms involving only properties of the granular system.

σ_n = the normal pressure.

σ_3 = the lateral pressure in a standard triaxial test.

ϕ = the angle of internal friction.

$\tan\phi$ = the coefficient of internal friction.

$\tan\phi_e$ = the component of $\tan\phi$ due to interlocking.

$\tan\phi_{max}$ = the maximum $\tan\phi$ for a static test at an initial void ratio equal to the CVR.

$\tan\phi_{min}$ = the limiting minimum $\tan\phi$.

$\tan\phi_r$ = the component of $\tan\phi$ due to frictional resistance.

$\tan\phi_{st}$ = the maximum $\tan\phi$ for a static test at the void ratio in question.

$\tan\phi_{v}$ = the coefficient of internal friction for an EVR condition test.

$\tan\phi_{\infty}$ = an estimate of $\tan\phi_{min}$ obtained by extrapolating the $\tan\phi_{v}$ - η curve to a value of η approaching infinity.

ω = the frequency of vibration, radians per second.

XII. APPENDIX B. TEST DATA

1. EVR Condition Tests

Material	σ_n(psi)	f'(cps)	η	Tanϕ_m	e_v	e_c
1/16" balls	2.5	0	0		0.737	
		10	.72		.724	
		15	1.63		.685	
		30	2.17		.663	
		20	2.90		.663	
		40	3.85		.639	
		25	4.52		.630	
		50	6.03		.608	
		30	6.52		.629	
		35	8.86		.622	
		40	11.58		.615	
1/16" balls	10.0	0	0	0.511	0.735	0.734
		30	0.54	.481	.722	.722
		30	1.09	.451	.713	.712
		25	3.00	.336	.691	.691
		40	5.78	.306	.673	.679
		45	7.32	.252	.652	.655
		45	9.76	.244	.632	.645
		10	0.72		.721	
		15	1.63		.706	
		20	2.90		.690	
		25	4.52		.677	
		30	6.52		.660	
		35	8.86		.648	
		40	11.58		.638	
		45	14.67		.628	
1/16" balls	20.0	0	0	0.478	0.733	0.730
		30	0.54	.462	.719	.722
		30	1.09	.440	.716	.717
		25	3.00	.354	.694	.697
		40	5.78	.302	.683	.685
		45	7.32	.280	.670	.668
		45	9.76	.224	.655	.658
		30	2.17	.382	.705	.709
		30	3.25	.352	.699	.701
		30	4.34	.036	.688	.689
		30	5.43	.306	.674	.679
		30	6.52	.291	.665	.665
		25	4.52		.687	

Material	σ_n(psi)	f'(cps)	η	Tanϕ_m	e_v	e_c
		30	6.52		.672	
		35	8.86		.660	
		40	11.58		.646	
		45	14.67		.636	
1/16" balls	30.0	0	0	0.474	0.730	0.726
		30	0.54	.446	.720	.718
		30	1.09	.408	.727	.720
		25	3.00	.389	.707	.705
		40	5.78	.303	.682	.688
		45	7.32	.286	.659	.665
		45	9.76	.260	.663	.666
		25	4.52		.696	
		30	6.52		.679	
		35	8.86		.664	
		40	11.58		.651	
		45	14.67		.642	
1/16" balls	40.0	0	0	0.438	0.729	.723
		30	0.54	.426	.721	.718
		30	1.09	.425	.721	.721
		25	3.00	.382	.702	.705
		40	5.78	.325	.686	.692
		45	7.32	.292	.671	.674
		45	9.76	.248	.667	.667
		25	4.52		.697	
		30	6.52		.684	
		35	8.86		.673	
		40	11.58		.660	
		45	14.67		.644	
1/16" balls	50.0	0	0		.728	
		10	0.72		.726	
		15	1.63		.721	
		20	2.90		.715	
		25	4.52		.703	
		30	6.52		.692	
		35	8.86		.678	
		40	11.58		.663	
		45	14.67		.657	
		30	0.54		.725	
		30	1.09		.724	
		25	3.00		.712	
		40	5.78		.691	
		45	7.32		.676	
		45	9.76		.668	

Material	σ_n(psi)	f'(cps)	η	Tanϕ_m	e_v	e_c
3/32" balls	20.0	0	0	0.497	0.779	.784
		30	1.09	0.440	.753	.755
		25	3.00	-	.741	.739
		40	5.78	0.287	.703	.708
		45	9.76	0.191	.687	.690
		0	0		.766	
		10	0.48		.764	
		15	1.09		.759	
		20	1.93		.750	
		25	3.00		.740	
		30	4.34		.729	
		35	5.90		.718	
		40	7.71		.708	
		45	9.76		.696	
		50	12.20		.688	
		55	14.67		.674	
1/8" balls	20.0	0	0	0.497	.807	.809
		30	1.09	.392	.779	.779
		25	3.00	.335	.763	.769
		40	5.78	.268	.741	.751
		45	9.76	.182	.725	.736
		0	0		.793	
		10	0.43		.789	
		15	1.09		.782	
		20	1.93		.772	
		25	3.00		.760	
		30	4.34		.750	
		35	5.90		.742	
		40	7.71		.738	
		45	9.76		.730	
		50	12.20		.723	
		55	14.67		.716	
5/32" balls	20.0	0	0		0.829	
		10	0.48		.824	
		15	1.09		.815	
		20	1.93		.798	
		25	3.00		.787	
		30	4.34		.779	
		35	5.90		.767	
		40	7.71		.758	
		45	9.76		.751	
		50	12.20		.747	
		55	14.67		.745	

Material	σ_n (psi)	f' (cps)	η	Tanϕ_m	e_v	e_c
Sand	5.0	0	0		0.698	
		10	0.48		.689	
		15	1.09		.683	
		20	1.93		.665	
		25	3.00		.647	
		30	4.34		.630	
		35	5.90		.617	
		40	7.71		.594	
		45	12.08		.551	
		50	14.67		.532	
Sand	10.0	0	0	0.695	0.690	0.684
		20	0.96	.675	.659	.657
		40	1.93	.626	.649	.648
		60	4.34	.550	.614	.621
		35	8.86	.458	.595	.590
		50	12.08	.415	.576	.566
		0	0		.682	
		10	0.72		.672	
		15	1.63		.656	
		20	2.90		.643	
		25	4.52		.628	
		30	6.52		.613	
		35	8.86		.600	
		40	11.58		.584	
		45	14.67		.569	
Sand	19.1	0	0	0.704	.676	.678
		30	0.54	.690	.680	.679
		30	1.09	.680	.665	.663
		30	2.17	.660	.653	.660
		30	3.25	.616	.649	.652
		30	4.34	.584	.645	.643
		30	5.43	.570	.635	.632
		30	6.52	.560	.623	.618
Sand	20.0	0	0	0.677	0.690	0.691
		20	0.96	.650	.683	.678
		40	1.93	.607	.665	.662
		60	4.34	.581	.633	-
		35	8.86	.538	.617	.617
		50	12.08	.480	.594	.592
		0	0		.677	
		10	0.72		.671	
		15	1.63		.660	
		20	2.90		.648	

Material	σ_n(psi)	f'(cps)	η	Tanϕ_m	e_v	e_c
		25	4.52		.634	
		30	6.52		.621	
		35	8.86		.608	
		40	11.58		.591	
		45	14.67		.584	
Sand	40.0	0	0	0.655	.687	.682
		20	0.96	.650	.675	.673
		40	1.93	.625	.676	.673
		60	4.34	.584	.639	.639
		35	8.86	.561	.616	.620
		50	12.08	.530	.605	.605
		0	0		.674	
		10	0.72		.670	
		15	1.63		.663	
		20	2.90		.654	
		25	4.52		.640	
		30	6.52		.625	
		35	8.86		.614	
		40	11.58		.603	
		45	14.67		.584	
Sand	50.0	0			.681	
		10			.679	
		15			.671	
		20			.661	
		25			.654	
		30			.638	
		35			.625	
		40			.617	
		45			.606	

2. Non-EVR Condition Tests

Materials	σ_n(psi)	f'(cps)	η	e_o	$\tan\phi_m$	$\tan\phi_u$	$\tan\phi_r$	$\tan\phi_e$
1/16" balls	20.0	0	0	0.663	0.534	0.50	0.34	0.19
		30	0.54	.662	.497	.46	.33	.17
			1.09	.662	.482	.45	.32	.16
			2.17	.662	.425	.40	.33	.09
			3.25	.661	.383	.38	.26	.12
			4.34	.661	.363	.37	.28	.08
			5.43	.663	.324	.33	.25	.07
			6.52	.662	.291	.29	.24	.05
		0	0	.633	.570	.54	-	-
		30	0.54	.635	.555	.48	.33	.22
			1.09	.634	.525	.47	.29	.23
			2.17	.636	.498	.44	.29	.21
			3.25	.633	.420	.38	.24	.18
			4.34	.633	.382		.20	.18
			5.43	.630	.333	.29	.22	.11
			6.52	.633	.303	.29	.22	.08
		30	1.09	.684	.460	-		
		0	0	.687	.519	-		
			0	.713	.479	-		
1/16" balls	10.0		0	.662	.588	.53		
			.54		.544	.53		
			1.09		.520	.50		
			2.17		.450	.45		
			2.17		.428	-		
			2.17		.466	-		
			3.25		.382	.38		
			4.34		.340	.32		
			5.43		.324	.30		
			6.52		.306	.25		
	20.0		.97	.662	.484	.44		
			1.93		.451	.42		
			3.85		.358	.32		
			5.78		.302	.27		
			7.71		.258	.26		
			4.34		.333	.29		
			7.85		.272	.25		
			8.68		.254	.24		
			2.90		.387	.34		
			0.72		.515	-		

Materials	σ_n(psi)	f'(cps)	η	e_o	$\tan\phi_m$	$\tan\phi_u$	$\tan\phi_r$	$\tan\phi_e$
1/16" balls	40.0	0	0	.662	.500	.41		
		30	.54		.460	.41		
		30	1.09		.460	.40		
			2.17		.420	.40		
			3.25		.398	.39		
			4.34		.386	.33		
			5.43		.352	.32		
			6.52		.335	.29		
			0	.633	.555	.43		
			1.09		.505	.42		
			2.17		.457	-		
			3.25		.440	.43		
			4.34		.415	.38		
			5.43		.417	.38		
			6.52		.385	.32		
Sand	10.0	0	0	.612	.870	.78		
		20	.96	.612	.802	.72		
		40	1.93	.612	.697	.68		
		60	4.34	.610	.565	.55		
	20.0	0	0	.612	.860	.74	.71	.14
		20	.96	.612	.795	.66	.68	.12
		40	1.93	.612	.715	.64	.63	.09
		60	4.34	.612	.612	.57	.55	.06
		35	8.86	.612	.529	.53	.51	.02
	40.0	0	0	.61	.850	.66		
			.96		.801	.69		
			1.93		.776	.64		
			4.34		.645	.60		
			8.86		.604	.54		
	10.0	0	0	.581	.955	.40		
			.96	.583	.840	-		
			1.93	.584	.814	.57		
			4.34	.584	.600	.71		
			8.86	.584	.475	.72		
			12.08	.585	.442	.78		
	20.0	0	0	.584	.952	.77	.75	.20
			.96	.583	.851	.69	.71	.14
			1.93	.583	.725	.63	.65	.07
			4.34	.580	.615	.55	.54	.08
			8.86	.582	.564	.51	.51	.05
			12.08	.578	.490	.46	.48	.01

Material	σ_n (psi)	f' (cps)	η	e_o	$\tan\phi_m$	$\tan\phi_u$	$\tan\phi_r$	$\tan\phi_e$
Sand	40.0	0	0	.58	.933	.67		
			0.96		.900	.69		
			1.93		.846	.60		
			2.96		.770	.64		
			4.34		.680	.59		
			8.86		.612	.54		
			12.08		.565	.52		
Sand	19.1	0	0	.635	.776	.72		
				.608	.780	.71		
				.605	.776	.74		
				.578	.852	.71		
				.571	.856	.72		
				.562	.952	-		
				.545	1.080	.70		
		30	1.09	.640	.720	.70		
				.593	.736	.72		
				.563	.824	.68		
				.549	.950	-		
		30	2.17	.615	.688	.66		
				.563	.785	.66		
				.549	.836	.64		
		30	3.25	.640	.629	-		
				.567	.726	.63		
				.552	.793	-		
		30	4.34	.585	.704	.63		
				.550	.646	.58		
		30	5.43	.607	.598	.58		
				.585	.580	.58		
				.551	.646	.58		